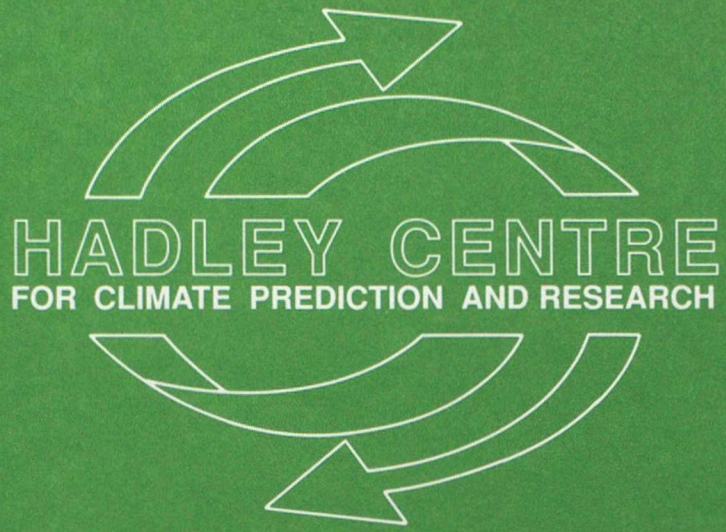

Modelling interannual variability in the Indian Ocean using momentum fluxes from the UKMO and ECMWF operational weather analyses.

by

D. L. T. Anderson and D. J. Carrington

CRTN 25 February 1992

CLIMATE
RESEARCH
TECHNICAL
NOTE

Hadley Centre
Meteorological Office
London Road
Bracknell
Berkshire RG12 2SY

CLIMATE RESEARCH TECHNICAL NOTE NO. 25

MODELLING INTERANNUAL VARIABILITY IN THE INDIAN OCEAN USING MOMENTUM FLUXES FROM THE UKMO AND ECMWF OPERATIONAL WEATHER ANALYSES

by

D L T ANDERSON

Clarendon Laboratory, Oxford

and

D J CARRINGTON

Hadley Centre

Hadley Centre for Climate Prediction and Research
Meteorological Office
London Road
Bracknell
Berkshire RG12 2SY
U.K.

Note: This paper has not been published. Permission to quote from it should be obtained from the Director of the Hadley Centre.

ABSTRACT

A 16-level general circulation model of the Indian ocean is used to reproduce interannual variability in ocean circulation from 1987 to 1990 using wind stress from the UKMO operational forecast model analyses. The results of this integration are compared with those obtained using the Hellerman and Rosenstein (HR) climatological forcing. The differences in the two wind products are large, as are the resulting surface and subsurface currents. Model results are compared with observations at 55°E and 73°E on the Equator. The undercurrent using UKMO stresses is more strongly eastward than that using HR, and in the four years studied the model always simulates an undercurrent in February-March at Gan (73°E), contrasting with the inconsistancy of its appearance in the years sampled by the observations. Interannual differences in the surface currents can be large, as much as 100 cms^{-1} in May on the Equator.

The years 1987 and 1988 are worthy of special consideration since 1987 was a drought year over India and 1988 had above average rainfall. Therefore, the period 1987/1988 is repeated using ECMWF stresses. Again there are large differences between these and the UKMO stresses and also in the resulting surface currents, where differences can be as much as 80 cms^{-1} over a large area of the equatorial zone and in the Somali current region. At undercurrent depth, the response at Gan (73°E) is very similar in the first half of the year in all three integrations, but differs significantly in the second half. In particular both the UKMO and ECMWF induce a semi-annual response, whereas HR leads to an annual cycle. Although interannual differences are large on a month to month basis, they are not long lasting.

Comparison is also made between the simulations of surface topography from the model and GEOSAT altimetry data. While there is broad scale similarity in pattern between the two simulations and the GEOSAT observations, detailed agreement between the fields is poor.

1. Introduction

The Tropical Ocean Global Atmosphere programme (TOGA) of the World Meteorological Organisation requires the development of coupled atmosphere ocean models. As a step towards this goal, the component models can be tested separately. Atmospheric models can be tested by verifying how well they reproduce climate variations when forced with prescribed Sea Surface Temperatures (SSTs). A parallel study would seem to be to run an ocean model forced by prescribed fluxes of momentum, heat and fresh water and to verify the model variables such as currents or SSTs. The former experiment is considerably easier to organise than the latter, because the forcing field (SST) is much better determined than the fluxes which are not known to an acceptable accuracy. Studies of the variability in the tropical oceans have often proceeded using the observed anomalies in only the momentum flux because the heat and fresh water fluxes are inaccurate. This is useful for studying the variability in the circulation, and may on occasion have wider applicability: for example almost all studies of the variability of SST in the equatorial Pacific have been of this form since the models are either adiabatic and so do not require a heat flux, or, if they are thermodynamically active, then the heat flux is parameterised as a form of negative feedback to observed or climatological SST.

In this study we consider variability in the currents of the Indian Ocean, using observed momentum fluxes from the operational numerical weather prediction model analyses of the UK Met Office (UKMO) and the European Centre for Medium Range Weather Forecasts (ECMWF). In a companion study the use of heat fluxes from the ECMWF analyses is considered (Carrington and Anderson 1992). For present purposes, the heat flux is obtained by relaxing SST back to climatological values with a time-scale of 50 days. This prevents a proper analysis of SST variability, since, in the Indian Ocean, changes in SST may be less closely tied to variations in thermocline depth and more dependent on surface heat fluxes than in the Pacific. It does however allow an analysis of the circulation field. Ideally one would like to compare the model output with observations, but current measurements for the 1987–1990 period in the Indian Ocean are almost totally lacking. Therefore interannual variations in currents are examined (section 2) but without any verification of their correctness. A simulation of the seasonal cycle of currents in the Indian Ocean in response to climatological forcing has been described in Anderson *et al.*, (1992).

The ocean is an inherently simpler system than the atmosphere in the sense that

variations in the circulation field depend much more on the forcing field than on the internal model dynamics or parameterisations. For that reason, it is instructive to compare the model results when forced with two different, but presumably realistic, wind fields. This is done in section 3, where the variability in the oceanic response for the years 1987 and 1988 to UKMO forcing is compared with the response to ECMWF forcing. This period was chosen as the years 1987 and 1988 have been singled out for special attention by the TOGA-MONEG† group since the former corresponds to a particularly weak monsoon and the latter to a strong one (as measured by rainfall over India).

The ocean model used has been described in Anderson *et al.*, (1992) and so will not be discussed in detail here, but briefly, it is a general circulation model with 16 levels in the vertical, of which 7 are in the upper 100 m. The latitudinal resolution varies from $\frac{1}{3}^\circ$ in the equatorial region to 1° at 30° from the equator while the longitudinal resolution varies from $\frac{1}{2}^\circ$ near the western boundary to $1\frac{1}{2}^\circ$ in the east.

Studies of the Indian Ocean using interannual forcing have also been conducted by Dube *et al.*, 1990. This paper complements their work in that independently derived wind forcing fields are used and the type of ocean model is different as well: viz an ocean GCM in this study as opposed to a reduced gravity model in Dube *et al.*. Although the model in this study has less horizontal resolution than that used by Dube *et al*, it has better vertical resolution allowing examination of variability in the subsurface flow as well as in the surface currents.

2. Results from integrations using UKMO analyses

2.1 The mean seasonal cycle

Analysed wind fields from operational weather forecast centres can differ markedly from published climatologies. This is illustrated in Fig. 1, in which the average seasonal cycle of zonal wind stress based on the 4 years 1986–1990 at (a) 55°E, taken as representative of the western region, and (b) 73°E, taken as representative of the central eastern region, is plotted (solid curve) for comparison with the seasonal cycle of zonal stress from Hellerman and Rosenstein (1983) shown by the dashed curve. The longitudes 55°E and 73°E correspond to two sites where most data for the Indian ocean have been collected (see Leetmaa and Stommel 1980 who collected two years of Spring data at 55°E and Knox

† *MONEG Monsoon Numerical Experimentation Group is a subgroup of the TOGA programme devoted to understanding and modelling of the monsoon, particularly the summer monsoon of the Indian Sub-Continent.*

1976 who collected $2\frac{1}{2}$ years of data at Gan, 73°E). At both locations, there are substantial differences between the forcing fields; for example the Hellerman and Rosenstein (HR) stresses are considerably stronger than the UKMO stresses, on average by about 0.02 Nm^{-2}. This variation is comparable to the amplitude of the seasonal cycle and is significant in terms of the equatorial ocean currents it can drive. Also shown are the analysed values for the individual years 1987–90. At both locations the HR stresses lie outside the interannual variability range for much of the year.

In fig. 2 the mean seasonal cycle of surface zonal currents is plotted for the experiment forced by the UK Met. Office wind stresses, denoted INDG. At 55°E, the currents show a marked semi-annual cycle, with a mean which is *westward.* In May and November, there are eastward currents of strength 25 cm s^{-1} and 40 cm s^{-1}, corresponding to the Wyrtki Jet (Wyrtki, 1973). This is stronger further to the east, as can be seen in fig. 2b for 73°E, where the Spring and Autumn speeds reach 50 cms^{-1} and 60 cms^{-1}. At this longitude the currents for INDG have an annual mean close to zero. The currents from the experiment in which the model was forced by HR stresses, denoted IND1 (described in Anderson *et al.*, 1992), are also shown for comparison. At both 55°E and 73°E, the currents are more eastward in experiment IND1 than in INDG, consistent with the stronger eastward wind stresses in the HR analysis.

The average seasonal zonal currents at 113 m (representative of the undercurrent depth) and the interannual variations in undercurrent strength at 73°E are plotted in fig. 3. Whereas there were large differences in the surface currents between IND1 and INDG, these differences are somewhat smaller at undercurrent depth particularly in the first 6 months of the year despite the large differences in wind stress. It is in the latter half of the year that the currents are most different. Comparison with fig. 1 shows that although the annual mean wind is not strongly eastwards in INDG, the mean current at 113 m *is.* Even though the wind is more strongly eastward in IND1 than in INDG, the mean current at 113 m is not.

Cane 1980, has shown that, in his model, when the ocean is in steady state both eastward and westward winds will give rise to eastward flow at undercurrent depth, albeit for different reasons. The ocean response is not just related to the local wind: it also depends on remote forcing via Kelvin and planetary waves. In the case of a westward wind stress, the undercurrent may be established non-locally by the development of a pressure gradient against the western boundary. The stronger the westward surface stress,

the stronger the eastward undercurrent. On the other hand, an eastward wind stress will drive an eastward surface flow, which can be transmitted to the subsurface by local vertical advection and mixing. A pressure gradient may be established of such a sign as to retard the eastward flow but may not be strong enough to offset the vertical exchange of momentum, resulting in a current which, at ~100 m, is still eastward although weaker than the surface current. It could be in the opposite direction to the surface flow if the pressure gradient were stronger than the local vertical transfer terms. The winds change so rapidly in the Indian ocean, that the ocean is never in a state of equilibrium so the above pseudo-equilibrium arguments do not strictly apply but may nonetheless indicate why the ocean has a preference for eastward subsurface flow.

At 73°E, there are, in INDG, two periods of conventional undercurrent (eastward flow at ~100 m below westward surface flow): viz January-March and August-September. In IND1 the tendency to produce westward flow at ~100 m depth in June, July and August gives rise to a reverse undercurrent (westward flow at depth beneath an eastward surface flow). There are no occurrences of reverse undercurrents in the seasonally averaged cycle of INDG at 73°E other than a very weak occurrence in December. (The flow at 113 m is weakly westward in June and July but so too is the surface flow). At 55°E, the flow at 113 m is never westward in INDG so no reverse undercurrents occur there (not shown).

The seasonal cycle of currents observed at Gan is shown in fig. 4 from Reverdin 1987, based on Knox 1976. The surface flow in INDG (fig. 2b) is weak at the height of the Wyrtki jet in May and November compared to Knox's observations although broadly comparable at other times. The flow at the 20°C level (~100 m) is qualitatively similar to the model results shown in fig. 3 although there are specific differences; for example there is a one month phase-lag between the occurrences of extrema in the modelled and observed speeds (model leading). The strength of the modelled extrema are 40, -10, 20 and -10 cms/s, occurring in March, June, October and December compared to, 60, -10, 50, -15 cms/s occurring in April, July, November and January. The strength of the modelled eastward flow shows the greatest disagreement with Knox's measurements from September to November. The observations show a semi annual signal in undercurrent strength, as does INDG. By contrast, IND1 shows only an annual response.

The modelled phase of the surface flow in INDG fits that of the observations quite well and so the shear between the surface and undercurrent is larger in the model results. The modelled undercurrent extrema lead the surface by 1–2 months. There is an indication of

the undercurrent leading the surface in the observations also in the first half of the year.

2.2 Interannual variations

Fig. 1 gives an indication of the amplitude of interannual variations in zonal wind stress compared with the annual cycle. The corresponding interannual variations in zonal currents along the equator (fig. 2 and expanded in fig. 5) are (up to $\pm$ 50 cms^{-1}), comparable to the strength of the seasonal cycle itself (shown by the dashed line which corresponds to the average of the four years 1987–90 in INDG). In 1987, the currents were anomalously westward in the first part of the year until June, when they became anomalously eastward. In 1988, the anomalies were almost the opposite of the 1987 ones. In 1989 and 1990 the anomalous currents changed less from month to month, being usually less than 25 cm s^{-1}.

So far we have concentrated on variations in the equatorial region. To show the changes basin-wide the differences in surface currents between May 88 and May 87 from INDG are plotted in fig. 6a which shows that the largest changes are confined to the equatorial region, to the Sri Lankan current and to the Somali coast, with the Somali current being over 60 cms^{-1} stronger in May 88 than in May 87. By June, however, a somewhat different picture emerges (see fig. 6b) which indicates that the changes in strength have not been maintained. The Somali current is, if anything, weaker in June 88 than in June 87. In the equatorial region the currents in INDG are westward in June 88 while they are still eastward in June 87 (see fig. 5) giving rise to a westward anomaly. Another region of strong current is the Sri Lankan current, which flows strongly eastward, more strongly in 1988 than 1987.

Figs. 2 and 5 show that in both 1987 and 1988, all the key currents of the semi-annual cycle are present in both years, but they vary in strength and timing. Thus the Wyrtki Jet is most pronounced in May in 1988, while its maximum occurs later and is weaker in 1987. Likewise the westward flow in summer occurs earlier, in July 1988 compared to August in 1987. Interannual variability therefore occurs partly as a result of differences in timing as well as strengths of the wind field, and a few weeks is a long time in an ocean dominated by the semi-annual cycle. Outside the above regions, the interannual variation is smaller but in the South Equatorial Current it can reach 20 cm s^{-1}, which is comparable to the mean value there.

The interannual changes are not confined to the upper layers. Fig. 7 shows that differences in the zonal currents at 666 m can be up to 8 cms^{-1}, an indication that wind forcing is penetrating to this depth. As in Anderson *et al.*, (1992) the signal shows a

marked upward phase propagation. In each year there are two occurrences of eastward flow at 100 m although there is substantial interannual variation in the strength of the flow. It is particularly weak in September–October 1990.

The only long record of sub-surface currents in the Indian Ocean is at Gan taken by Knox 1976 who states that the record showed an undercurrent in February–March 1973, no undercurrent in 1974 and an undercurrent in February–March 1975, suggesting that the undercurrent does not always appear. Eastward flow is prevalent throughout the year except in July–August 1973 and July–August 1974 and in February–March 1974 when it was quite strongly westward. Fig. 7 and fig. 3 never show a westward current at 113 m in February–March. Whether this is because we have not sampled sufficient variability (4 years) or whether it reflects a deficiency in the forcing in the model is unresolved. Latter in sec 3, we will use ECMWF stresses. In this case, too there is no westward flow in February and March.

The signal at 666 m on the Equator propagates strongly from east to west (not shown) in a manner similar to that in Anderson *et al.* (1992). In contrast, the dynamic topography at 113 m (not shown) and at the surface (fig. 8a) show west to east propagation through the central Indian ocean, with stationary phase in both the west and east. Interannual changes in surface dynamic height in the central equatorial area are up to $\pm$ 5 dyn cms but further east the variability can be several dyn cms larger.

In order to distinguish the variability of seasonal from interannual changes, we define a seasonal range, equal to the difference between the maximum and minimum monthly mean dynamic height in the 4 year mean seasonal cycle from INDG which is shown in fig. 8b. The seasonal range is largest in the vicinity of the Somali gyre ($>$ 30 dyn. cms) but there are four large regions where the range is above 15 dyn. cms (excluding the large values along the eastern and southern boundaries), viz the Arabian Sea, Bay of Bengal, and the western and eastern equatorial zone. There are also regions where the modelled seasonal range is small, notably the central equatorial zone and much of the central Indian Ocean south of 10°S.

To give a measure of interannual variability, an interannual range was defined which is the difference between the maximum and minimum monthly mean dynamic height for that month during 1987–1990. This is shown in fig. 8c for July. In the equatorial zone as well as in the region 20° to the east of Madagascar, the interannual variability is comparable to or exceeds the seasonal range. In the Somali region, by contrast, the interannual range

is 6–8 dyn. cms., much smaller than the seasonal range.

A comparison of the model simulations was made with GEOSAT data. The seasonal range of GEOSAT data is shown in fig. 8d for comparison with fig. 8b. It is only weakly comparable over much of the field. In the central equatorial region, values of 6–8 dyn cms occur in both with higher values to the east and west. The high variability regions – the Western Arabian Sea, with a band from Kenya to India, the region to the northeast of Madagascar, and the region 10°S, 80–100°E – are present in both, but the details are different. The largest feature in fig. 8d is the region at 10°S, 80–100°E where the GEOSAT seasonal range is up to 28 cms, compared to the model range of only 12 dyn cms. On the other hand the variability in the Somali gyre reaches 32 dyn cms in the model compared with 20 cms in the GEOSAT data.

Interannual variability in the GEOSAT data (not shown) is much noisier than in the model (fig. 8c). The region east of Madagascar stands out, with values comparable to those modelled, but there is also a maximum in the GEOSAT data near 10°S, 90°E which is not present in the model results. The variability is higher in the Somali region (20 cm) compared to ~6 cm in the model. Overall, one can say there is some qualitative agreement between the two, but quantitatively they are rather different, most noticeably in the region 10°S, 80–90°E. Whether this illustrates a serious deficiency in the wind forcing used in the models is unclear. [Later, fig. 13 shows that this is a region where differences between the results using UKMO and ECMWF forcing are ~4 cm, small compared with the differences between model and observations.]

3. Results from integrations using ECMWF analyses

In addition to using UKMO forcing, a two year parallel integration has been performed using ECMWF momentum fluxes for the years 1987 and 1988, denoted INDN. Whereas the data used in the UKMO runs were 3 day averages, the stresses used in this section are derived from monthly averages by linear interpolation every 3 days.

The ECMWF stress fields on the Equator are qualitatively similar to the UKMO fields, but there are quantitative differences, shown in fig. 9a. Taking 1987 and 1988 as a whole the differences are at about the 0.01 Nm^{-2} level, smaller than the differences between the UKMO and HR fields and smaller than the size of the interannual differences themselves. There are occasions, however, when the differences are quite large (up $\pm 0.03 Nm^{-2}$): for example August 1987 and June 1988, both times when the UKMO stresses are strongly westward, and December 1987 and May 1988, when the UKMO stresses are strongly

eastward. Fig. 10 shows the actual stresses, from UKMO and ECMWF, at 73°E, where it can be seen that the UKMO stresses show greater variability and a stronger westward component especially in the northern hemisphere summer.

In neither of the two years 1973, 1974 (Knox 1976), nor in the HR climatology, were there strong westward stresses in the Northern Hemisphere summer at 73°E as exhibited by the UKMO analyses (see fig. 1 for example). The presence of a westward wind bias in the UKMO fields with respect to the ECMWF fields is even more noticeable further east (fig. 9a). Not surprisingly these stress differences can cause large differences in modelled currents. Fig. 9b shows the differences between the ECMWF and the UKMO surface zonal currents along the equator over a 2 year period. Averaged over the two years there is not a large bias in surface current strengths between INDG and INDN over $\frac{2}{3}$ of the basin but there is a bias in the eastern sector with INDG currents being less strongly eastward. July 1988 (see fig. 11) is one time when the differences are particularly large, with differences in equatorial currents between INDG and INDN of almost 1 ms^{-1}. The regions of greatest difference between INDG and INDN currents are the same as those where the interannual differences are largest, i.e. the equatorial zone, Sri Lankan and Somali currents.

Part of the differences in the Somali region illustrate a bias between the wind stresses in this area. The ECMWF winds drive more of a two-gyre circulation while the UKMO winds induce more of a continuous long-shore flow. The two gyre structure is frequently observed and thought to be the norm, suggesting that the ECMWF winds are preferable in this region although there are no observations to confirm this for the specific case of July 1988. In both INDG and INDN, the equatorial flow is westward, with the region of maximum currents around 70°E, but the INDG currents are substantially stronger.

The subsurface zonal currents are also different between experiments INDG and INDN as fig. 12 shows. The differences in UC strength are most evident in the second half of the year when they are comparable to interannual changes. There also appears to be a bias in the second half of the year, with INDG currents showing a stronger eastward flow than INDN currents. This difference is remarkably similar to that shown in Fig. 3 between the currents in INDG and IND1. The UKMO stresses are substantially more westward in the Northern Hemisphere summer than the ECMWF stresses which results in a stronger eastward sub-surface flow in INDG compared to either IND1 or INDN.

Turning to dynamic height, fig. 13a, shows the GEOSAT deviations from an annual mean and fig. 13b,c the model equivalents for July 88. There appears to be some broad

scale agreement between fig. 13b, c and even some correspondence between specific model features and GEOSAT. For example the large negative anomaly observed at 10°S, 90°E is weakly present in fig. 13b, while that at 18°S, 65°E is very weakly present in fig. 13c but the anomaly at 10°S, 90°E is not. Quantitative agreement is however, generally poor. The differences between the modelled fields are shown in fig. 13d. They are largest in the region of the Somali gyre mentioned earlier where they can reach 16 dyn cms and in the zone at 5°S where differences exceed 10 dyn cms. There are several areas where the differences are 4-6 dyn cms but south of 20°S the differences are small. These differences are in general not insignificant compared with the interannual changes (see fig. 8c), and in the case of the Somali gyre are several times larger.

Finally we consider SST changes. It has been possible to model interannual variability in SST in the tropical Pacific ocean using only the observed wind fields and a negative feedback to climatological SST to mimic heat flux. Even in the sub-tropics, there has been some partial success using only the momentum flux (Haney 1986). Can such a strategy work in the Indian ocean? To consider this question the differences in SST between July 1988 and July 1987 are shown in fig. 14 for (a) INDG and (b) INDN. These runs used the 'observed' momentum flux with a feedback to SST to minic heat flux with a relaxation time of 50 days. (See Anderson et al 1992 for a more specific description of the heat flux parameterisation). For comparison the differences in the observed SST's from the Climate Analysis Centre analysis for July 88 and July 87 are shown in fig. 14c.

Interannual variability in the Indian ocean is much smaller than in the Pacific so it is probably unlikely that a clear wind-driven signal would emerge. Comparing figs. 14a and 14b shows that this is indeed the case. There is some agreement between INDG and INDN in that the eastern equatorial region is warmer in 1988 and the western area and Somali basin cooler, but there is little agreement in detail or magnitude and neither agrees with the observations in fig. 14c. Qualitative comparison for other months supports the conclusion that the wind-driven variations in SST are not a good indicator of interannual variability in SST in the Indian ocean.

4. Summary

A four year integration of a model of the Indian Ocean has been made using stresses from the UK Met. Office operational analysis–forecast system from 1987–1990 and a two year integration for 1987–88 using ECMWF stresses. Table 1 summarizes the main features of the two integrations. The two years 1987–88 are of special interest since 1987 was a warm phase of the ENSO cycle when Indian monsoon rainfall was particularly weak and 1988 represented a strong cold phase of ENSO when the monsoon rainfall was above average.

There are large differences in the analyzed stresses both between years and between the two separate analyses. For example, the westerly stresses in May 1988 were particularly strong, both in the UKMO and the ECMWF analyses. By contrast, they were somewhat stronger than usual in November–December 87 according to the UKMO but not according to ECMWF. In general the level of difference between the two analyses in the Equatorial region is about 0.01 Nm^{-2}, but can be up to 0.03 Nm^{-2}, of similar size to the interannual differences. There is a relative bias between the two analyses, with the UKMO stresses consistently more easterly in the eastern part of the basin.

The stress differences, both interannual and between UKMO and ECMWF fields, can cause large differences in modelled surface currents particularly in the equatorial, Sri Lankan and Somali Current regions. Interannual differences in equatorial currents can be almost 1 ms^{-1} and in the Somali current region over 60 cms^{-1}; these are a result of differences in relative phase as well as in amplitude of the semi-annual and annual cycles in wind stress which dominate the equatorial and Somali regions respectively. The equatorial zonal current differences at the surface between the experiments using UKMO and ECMWF forcing (experiments INDG and INDN) can be as large as 80 cm s^{-1}, comparable to the size of interannual variations.

At equatorial undercurrent depth (~100 m), the interannual current variations are smaller, but are still substantial at ~40 cm s^{-1}. For example, in January 1987 (fig. 12) the flow was strongly eastward, but in January 1988 it was westward. The current at 113 m has an interesting seasonal cycle. Comparison of the 4 year UKMO seasonal cycle integration (INDG) with the seasonal cycle using climatological stresses (IND1) shows that a stronger eastward subsurface flow results in the former case although the UKMO stresses are less strongly eastward. Comparison of the years 1987, 1988 shows that the undercurrents obtained using UKMO stresses are also more strongly eastward than those

forced with the ECMWF stresses. The interannual variability extends to depths greater than 666 m, where peak to peak changes are $\sim$8 cm s^{-1}.

There are some features in the model simulations which are consistent with, and some which are inconsistent with Knox's record at Gan. The surface currents are generally similar. There are also similarities in the interannual differences in the undercurrent; for example, the lack of eastward flow in the model simulation of January 1988 mentioned above is somewhat similar to Knox's observations of 1974, although the absence of eastward flow was longer lasting in Knox's case, the current not becoming eastward until the end of March. A significant difference between the model and observations is that there can be strong shear in the model between the surface currents and those at 113 m, whereas the observations show in general a much stronger positive correlation.

One would like to be able to say that one wind product, UKMO or ECMWF, produced better-simulated currents than the other, but this is difficult to do since there are few ocean observations from 1987 or 1988 with which to compare. Some general remarks can be made, however. The Somali current shows a stronger two-gyre structure, more realistic in general, using ECMWF stresses than using UKMO stresses. The current at 113 m is more strongly eastward in August-October in the experiment using UKMO stresses in agreement with Knox's measurements for 1973 and 1974, whereas it is only weakly eastward when forced by ECMWF stresses. Comparison of dynamic height with the limited GEOSAT data fails to allow a good discrimination in the quality of the two flux products.

References

Anderson, David L.T., D. Carrington, R. Corry and C. Gordon (1992). The temporal evolution of Equatorial Currents in the Indian Ocean. Meteorological Office Climate Research Technical note.

Cane, M., (1980). On the dynamics of equatorial currents, with applications to the Indian Ocean. Deep Sea Res. 27A, *525-4*.

Carrington, D.J., and David L.T. Anderson (1992). Using an ocean model to validate heat fluxes from atmospheric models in operational and climate mode. In preparation.

Dube, S.K., M.E. Luther and J.J. O'Brien (1990). Relationships between interannual variability in the Arabian Sea and Indian Summer Monsoon. Meteorol. Atmos. Phys. 44, *153-165*.

Esbensen, S.K., and Y. Kushnir (1981). The heat budget of the global ocean: An atlas based on estimates from surface marine observations. Report No. 29, Climate Research Institute, Oregon State University, Corvallis.

Haney, R.L. (1985). Mid latitude sea surface temperature anomalies: a numerical hindcast. *J. Phys. Ocean*, **15**, *787-799*.

Hellerman, S., and M. Rosenstein (1983). Normal monthly wind stress over the world ocean with error estimates. J. Phys. Ocean, 13, *1093-1104*.

Knox, R., (1976). On a long series of measurements of Indian Ocean equatorial currents near Addu Atoll. Deep Sea Res. 23, *211-221*.

Leetmaa, A., and H. Stommel (1980). Equatorial current observations in the western Indian Ocean in 1975 and 1976. J. Phys. Ocean. 10, *258-269*.

Luksch, V., H. von Storch, E. Maier Reimer (1989). Modelling North Pacific SST anomalies as a response to anomalous atmospheric forcing. Max Plank Inst. fur Meteorologie Report No. 37.

Reverdin, G., (1987). The upper equatorial Indian Ocean: the climatological seasonal cycle. J. Phys. Ocean 17, *903-927.*

Wyrtki, K., (1973). An equatorial jet in the Indian Ocean. Science 181, *262-264.*

Table 1

Experiment	Forcing	Equatorial Stresses	Equatorial Currents	Somali Current
INDG	UKMO 1987-1990	Biased westward relative to ECMWF & HR, especially in the east	Surface currents more strongly westward than INDN or IND1 Stronger eastward under-current than INDN or IND1 Reverse UC unlikely	Single gyre
INDN	ECMWF 1987, 88	Weaker than HR	Reverse UC develops in summer as in Knox and in IND1 (IND1 is a seasonal cycle integration using HR wind stresses, described in Anderson et al. 1992)	Double gyre as is observed to be the norm, and as develops in IND1

Table 1 (cont.)

SST	Dynamic Topography
Shows large warm anomaly in east equatorial Indian Ocean in 1988. (Not observed in CAC)	Seasonal cycle gives changes of up to 30 cms in Somali region and 18 cms in eastern equatorial zone. Small signal in central southern IO. Interannual variations largest in eastern equatorial zone and east of Madagascar. Does not show large seasonal signal observed in GEOSAT data near 10° S, 80°-90° E.
Shows weak warm anomaly in east equatorial region in 1988. (Not observed in CAC)	Differences from INDG of up to 22 cms in Somali region. Large differences east of Madagascar and at 5° S. Does not show large seasonal signal observed in GEOSAT data near 10° S, 80°-90° E.

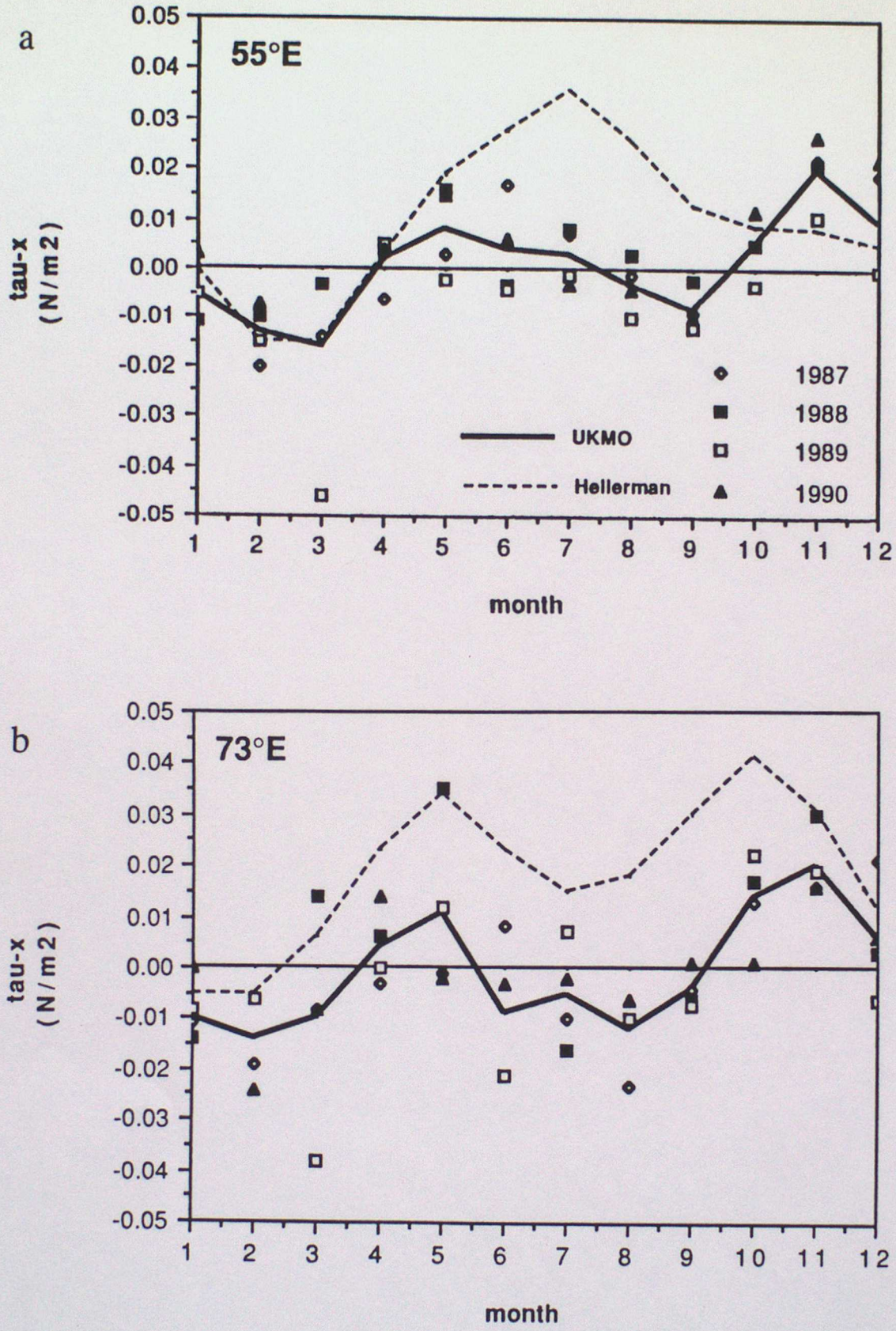

Fig. 1

Plot of the seasonal cycle of zonal wind from the UKMO analyses (solid curve), averaged over the 4 years 1987–1990 for (a) 55°E and (b) 73°E. For comparison, the seasonal cycle from Hellerman and Rosenstein (1983) is shown (dashed curve). There is a noticeable bias between the two wind products, with HR approximately 0.01 to 0.02 Nm^{-2} stronger on average. In order to show the range of interannual variability, the values for the individual years are also shown.

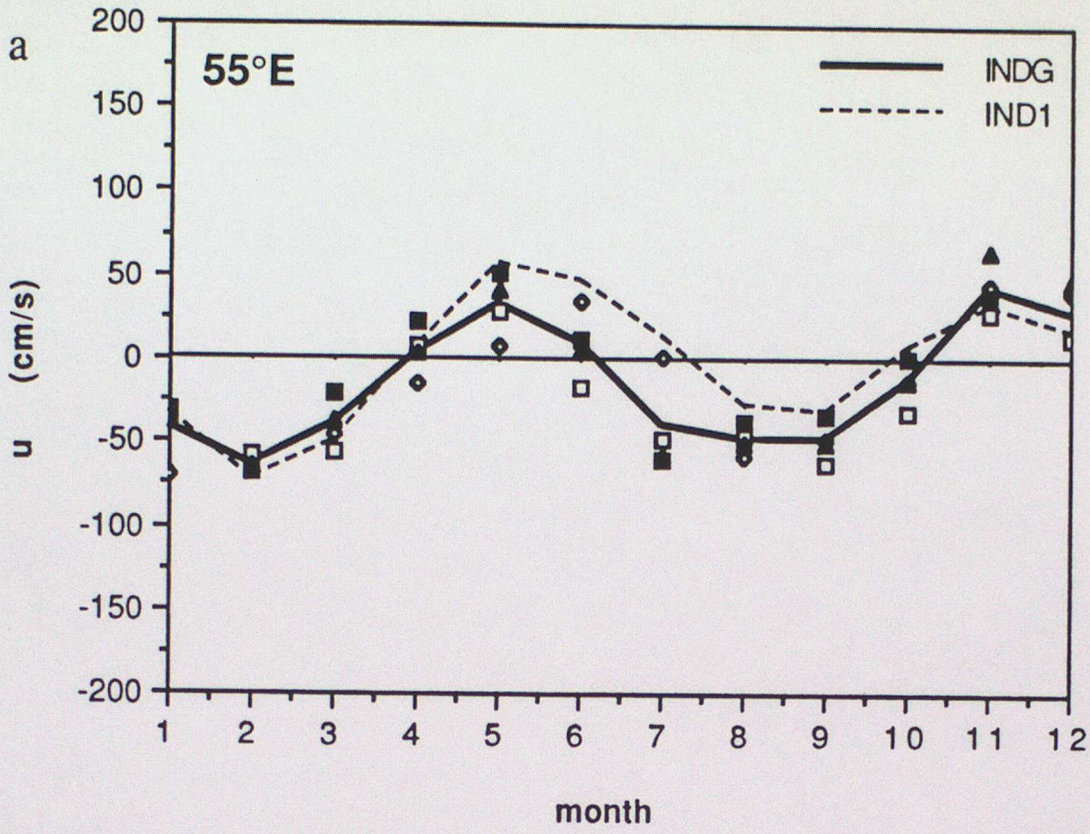

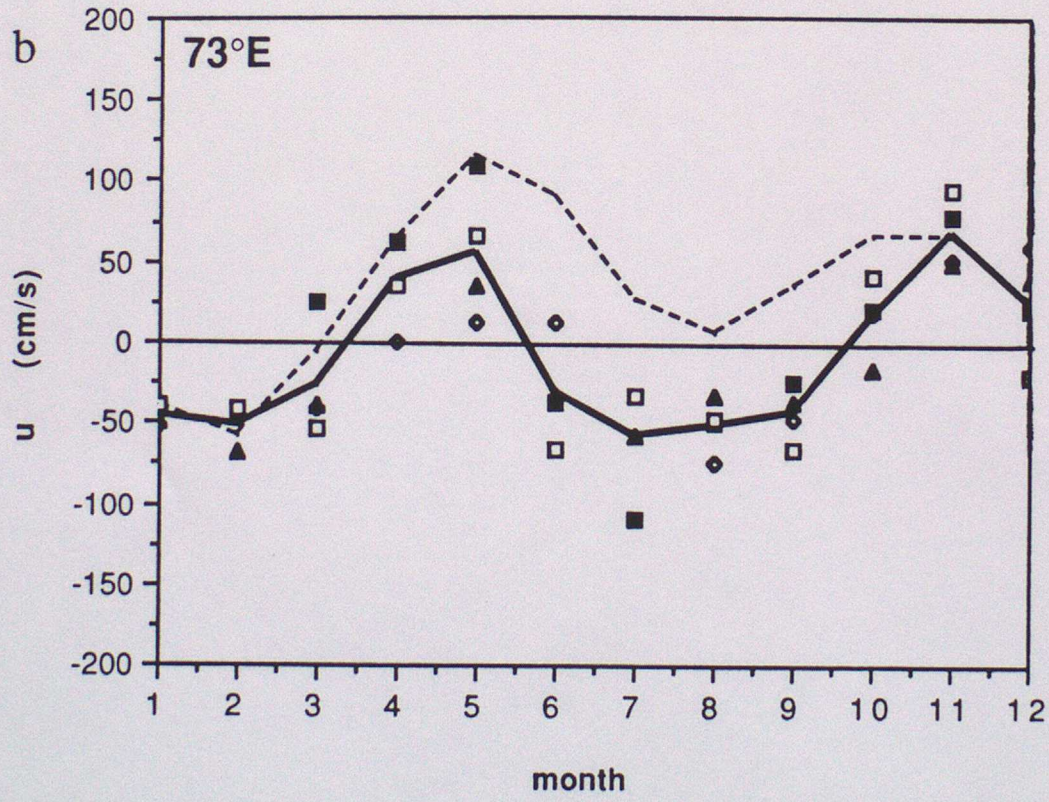

Fig. 2

Plot of the seasonal cycle of surface zonal currents from INDG (solid) and for IND1 (dashed), the former experiment corresponding to forcing by UK Met Office stresses and the latter to Hellerman and Rosenstein forcing, for (a) 55°E and (b) 73°E. The currents in IND1 are more strongly eastward than those in INDG consistent with the stronger eastward stresses of IND1. The currents for each month in the period 1987-90 are also shown, to indicate the range of interannual variability. This is typically around 50 cm/s, but can be as large as 100 cm/s in May and as small as 10 cm/s in January.

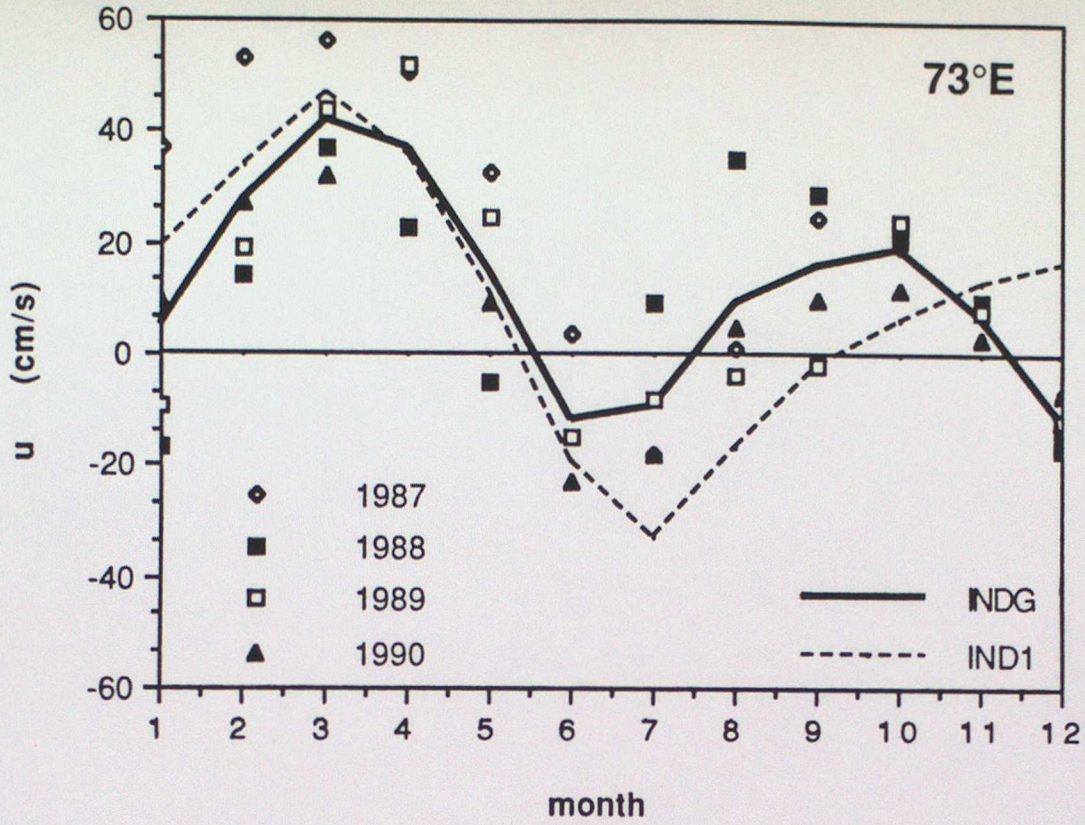

Fig. 3

The 4-year average seasonal cycle of zonal currents at 113 m at 73°E from INDG, compared with the seasonal cycle from IND1. The currents are rather similar over the first half of the year, but substantially different in the latter half. A conventional undercurrent is present in INDG from January-March and August-September. In IND1 there is a much stronger tendency to produce westward flow at 113 m in the June, July and August period which can give rise to a reverse undercurrent (westward flow at 113 m with eastward flow at the surface). INDG shows a marked semi-annual response, but that in IND1 is annual.

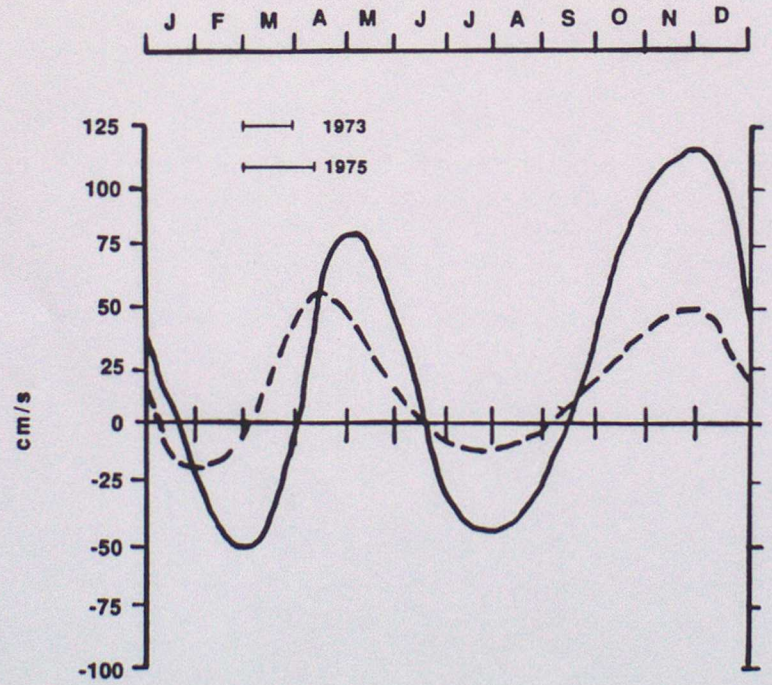

Fig. 4

Seasonal composite of currents from 90 profiles at Gan (73°E) for the period January 1973–June 1975 (Knox, 1976). The solid line is for currents averaged vertically in the mixed layer (average above the level with temperature one degree cooler than at 2 meter depth); dashed line for the currents at the 20°C level. The timing of the undercurrent is indicated in upper left of the diagram when known; it is earlier in INDG than in these observations. From Reverdin 1987. The timing of the undercurrent is earlier in INDG than in Fig. 4. There is a marked semi-annual response both at the surface and at ~100m, consistent with INDG but not IND1.

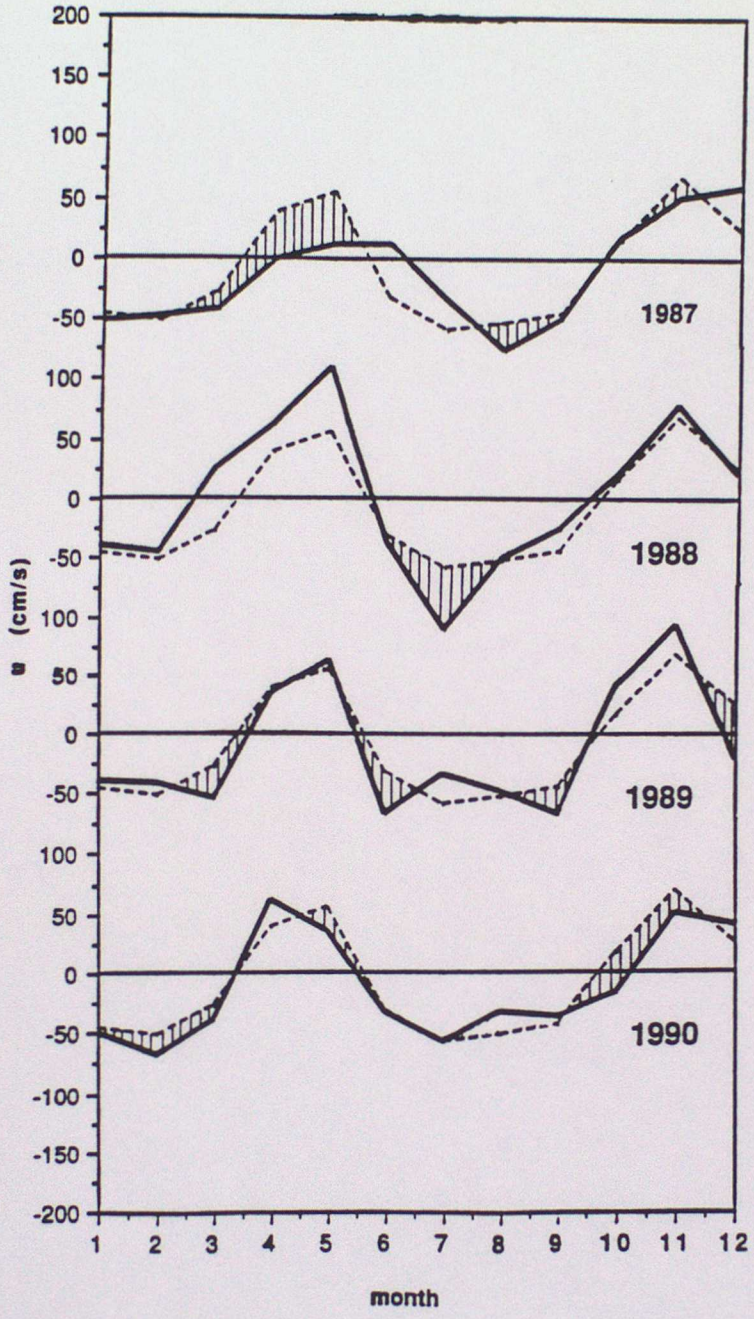

Fig. 5 Surface zonal currents at 73°E for (a) 1987, (b) 1988, (c) 1989 and (d) 1990 (solid curves), showing the very large differences between 1987 and 1988. The 4-year average currents are also shown (dashed). Shading indicates a westward anomaly with respect to this average.

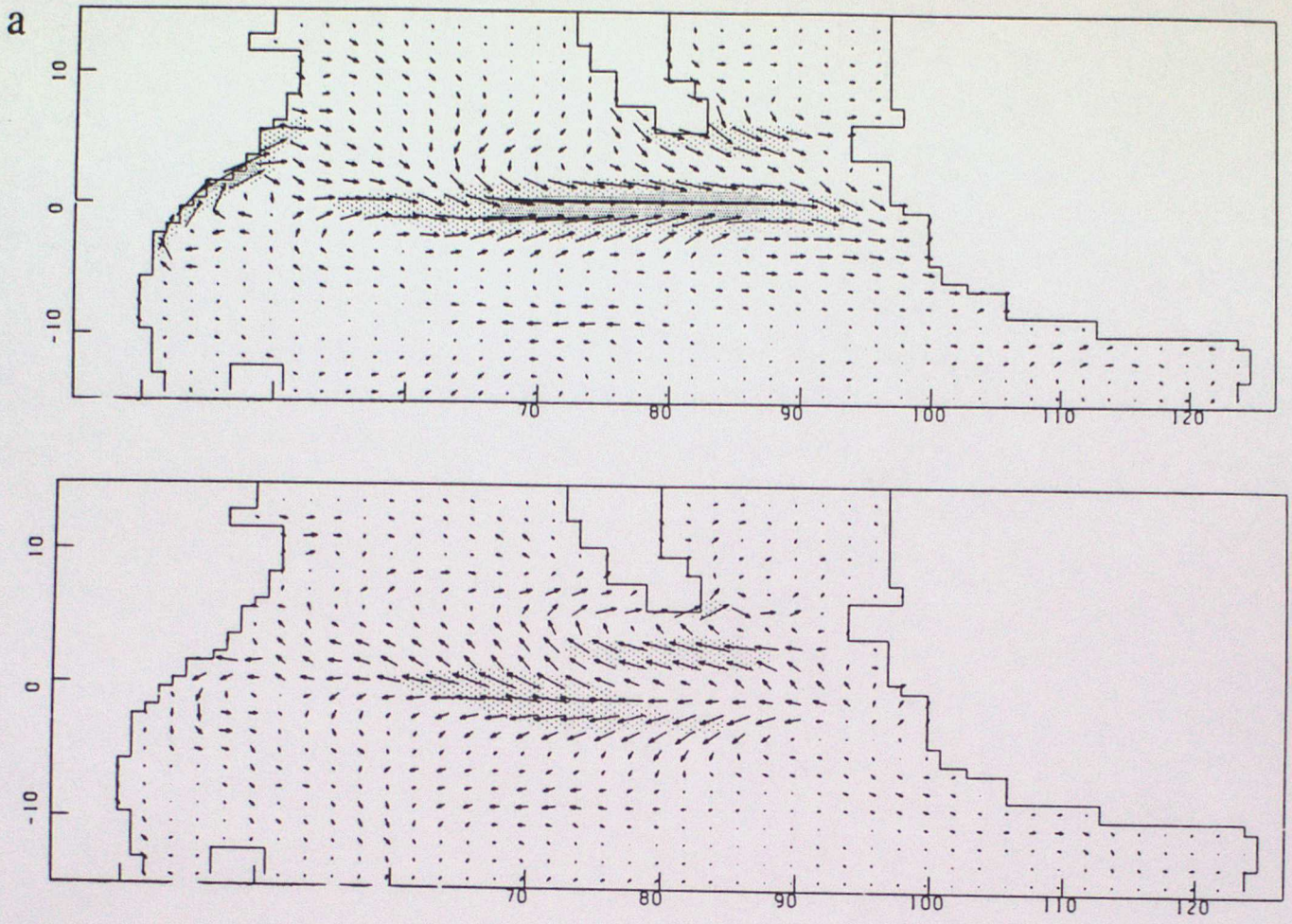

Fig. 6

The difference between surface currents in INDG (a) May 88–May 87 and (b) June 88–June 87. The differences are over 80 cm/s in the Somali current region and along the equator, and over 40 cm/s in the Sri Lankan current. Light shading indicates current differences between 40 cms^{-1} and 80 cms s^{-1}. Heavy shading indicates current differences greater than 80 cm s^{-1}. The sign of the difference changes between May and June.

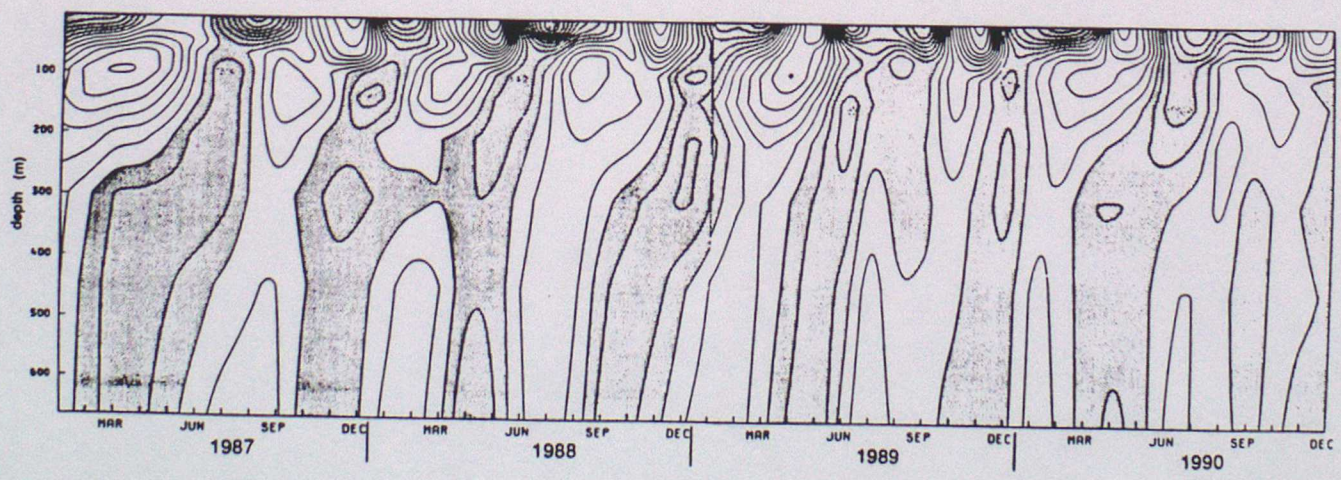

Fig. 7

Plot of the zonal currents at 73°E over the upper 666 m for the period 1987–1990, showing signs of upward phase velocity. At 666 m, the interannual variability is ~ 8 cm s^{-1}. In each year there are two occurrences of eastward flow at 100 m, although there is substantial variation in strength from year to year. The eastward flow is particularly weak in September-October 1990. The contour interval is 10 cms s^{-1}. Shading indicates westward velocities.

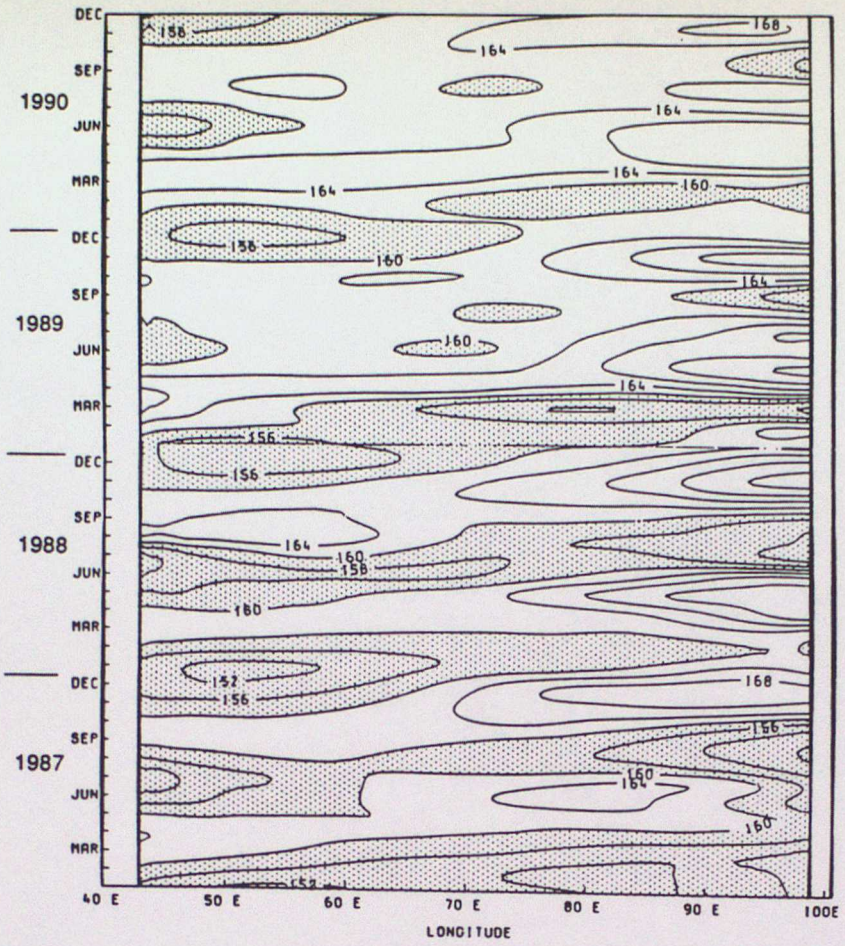

Fig. 8a

Contours of dynamic height (in dyn cm) along the equatorial section from 1987 to 1990 from INDG. The phase of the annual cycle is relatively stationery in both the western and eastern section, but changes rapidly in the central region. Interannual differences are approximately ± 5 dyn cms in the mid ocean but larger in the east.

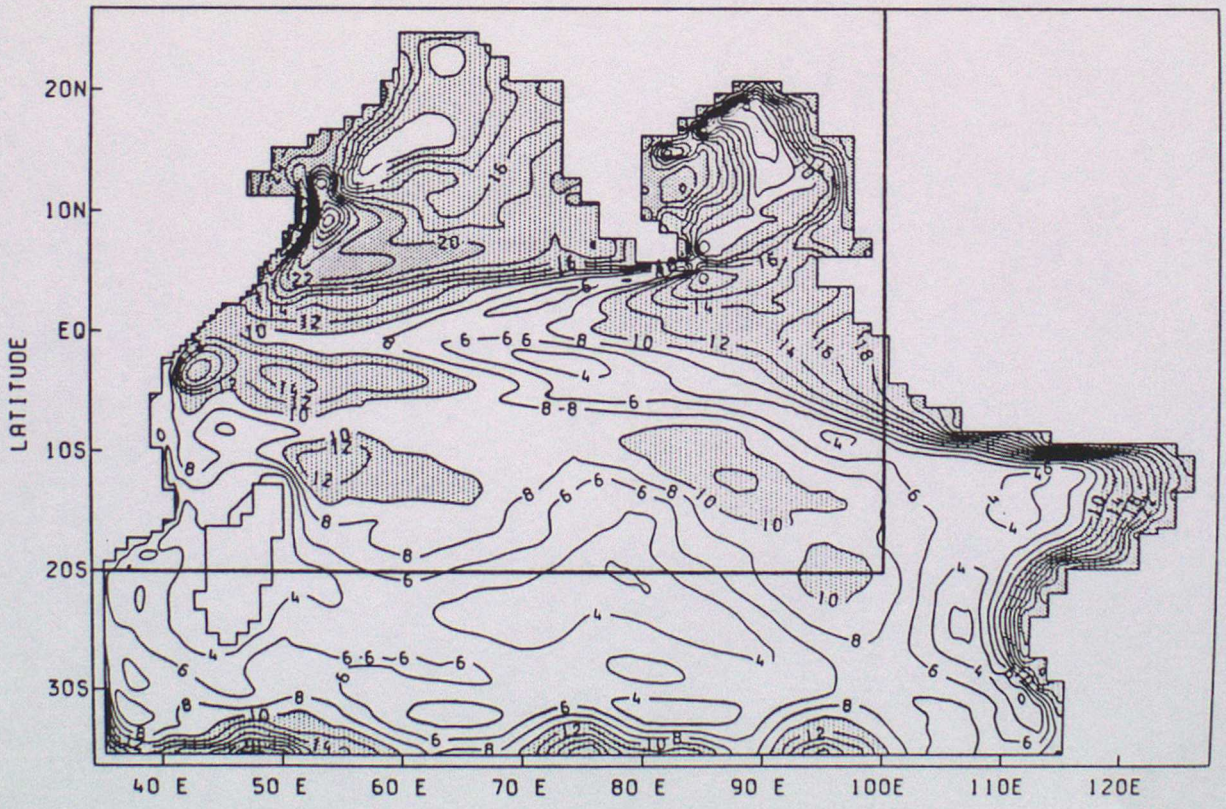

Fig. 8b

Contours of the seasonal range in dynamic height (in dyn cm) for INDG. The seasonal range is defined to be the difference between the largest and smallest values of monthly mean dynamic height at a point in the average seasonal cycle. The times of year in which these extremes occur may vary from place to place. The seasonal range is largest in the region of the Somali gyre. Solid lines at 20°S and 100°E correspond to the boundaries of the area of the GEOSAT data in fig. 8d.

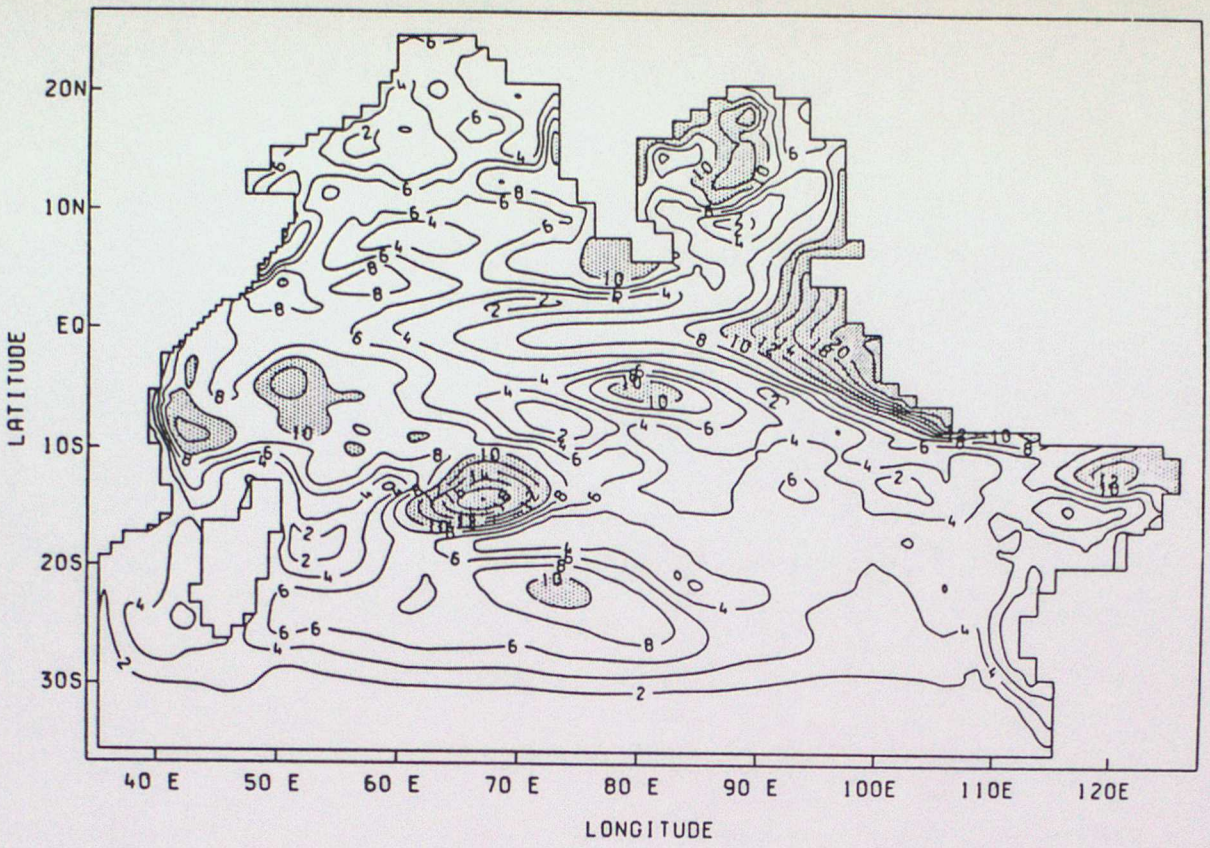

Fig. 8c

Contours of the interannual range in dynamic height (in dyn cm) in July for INDG. In the Somali region, Arabian Sea and most of the Bay of Bengal, the interannual range is significantly less than the seasonal range.

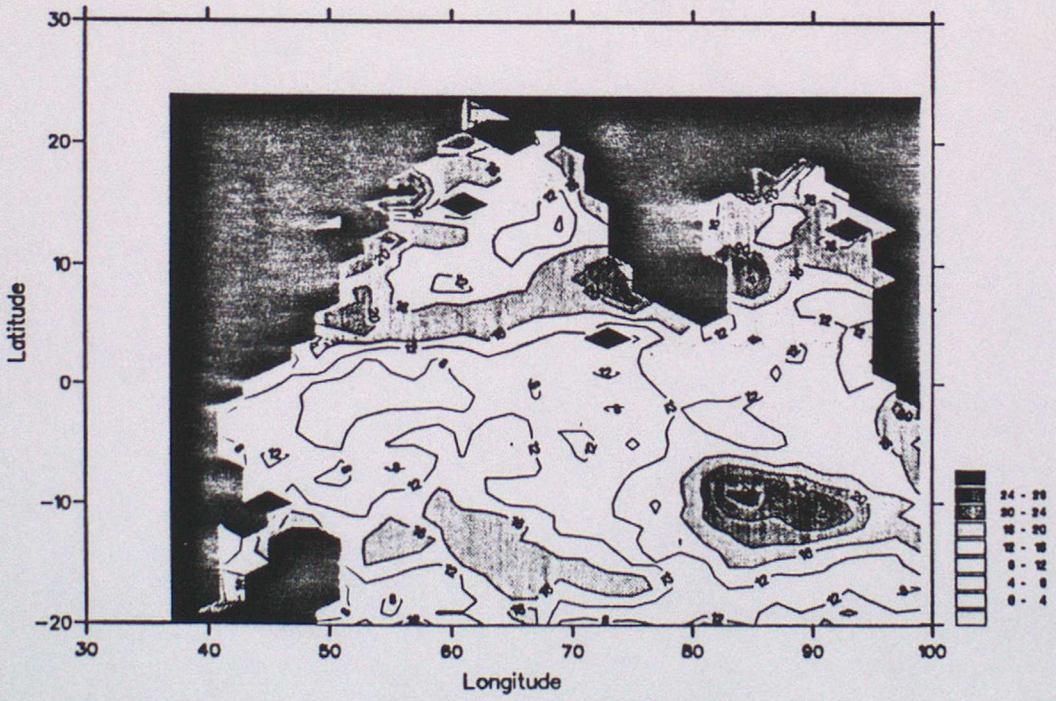

Fig. 8d

As for 8b, but for GEOSAT data. There is some broad scale agreement between fig. 8b and 8d but considerable variation in detail. A major maximum features in the GEOSAT data at 10°S, 80–90°E, which also occurs in INDG at this location but is much weaker. (Except for in this latter region, areas shaded black represent land or missing data).

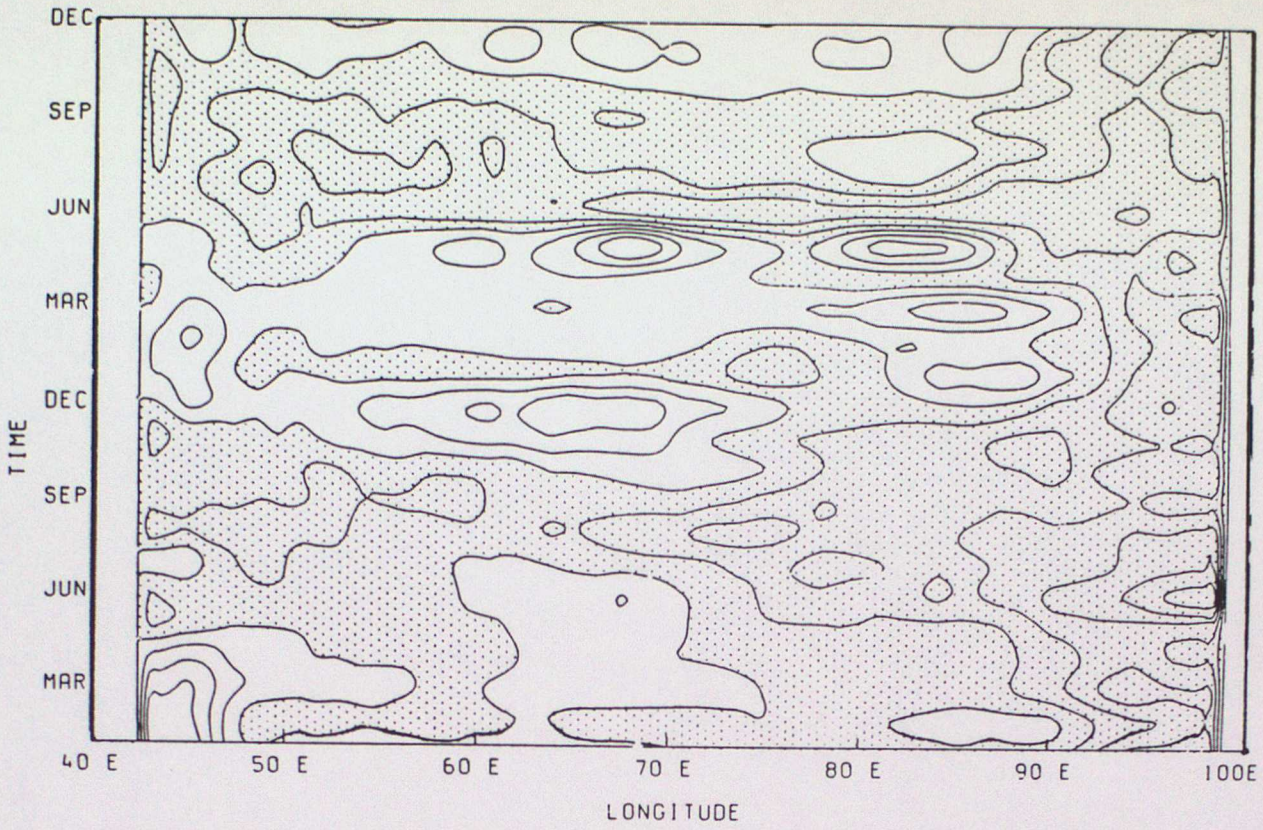

Fig. 9a

The difference in equatorial zonal wind stress (UKMO–ECMWF) over the period 1987 and 1988. Shading indicates negative values. The UKMO stresses have a considerable westward bias in the eastern third of the basin compared to the ECMWF stresses. The contour interval is 0.01 N/m^2.

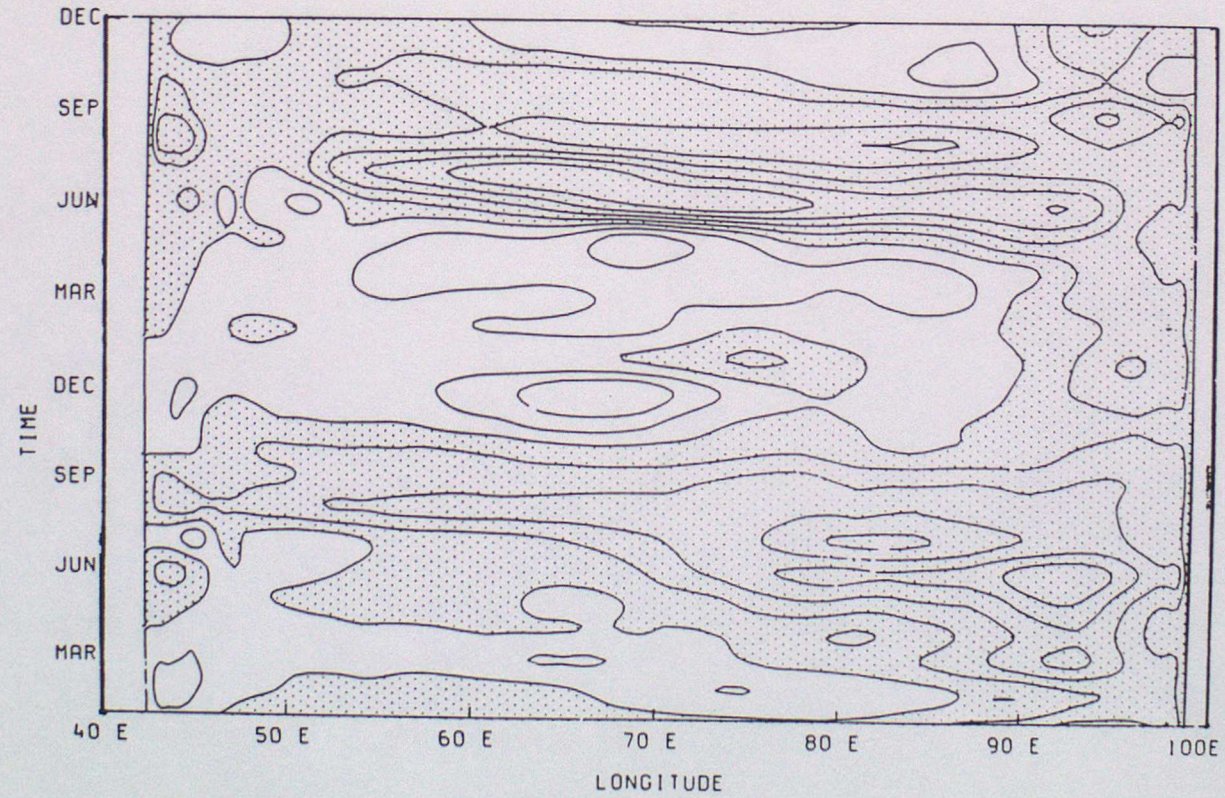

Fig. 9b

As for 9a but differences in surface zonal currents. Differences up to 80 cms^{-1} occur but 20 cms^{-1} is a more characteristic value. Contour interval is 20 cms^{-1}. Shading indicates negative values.

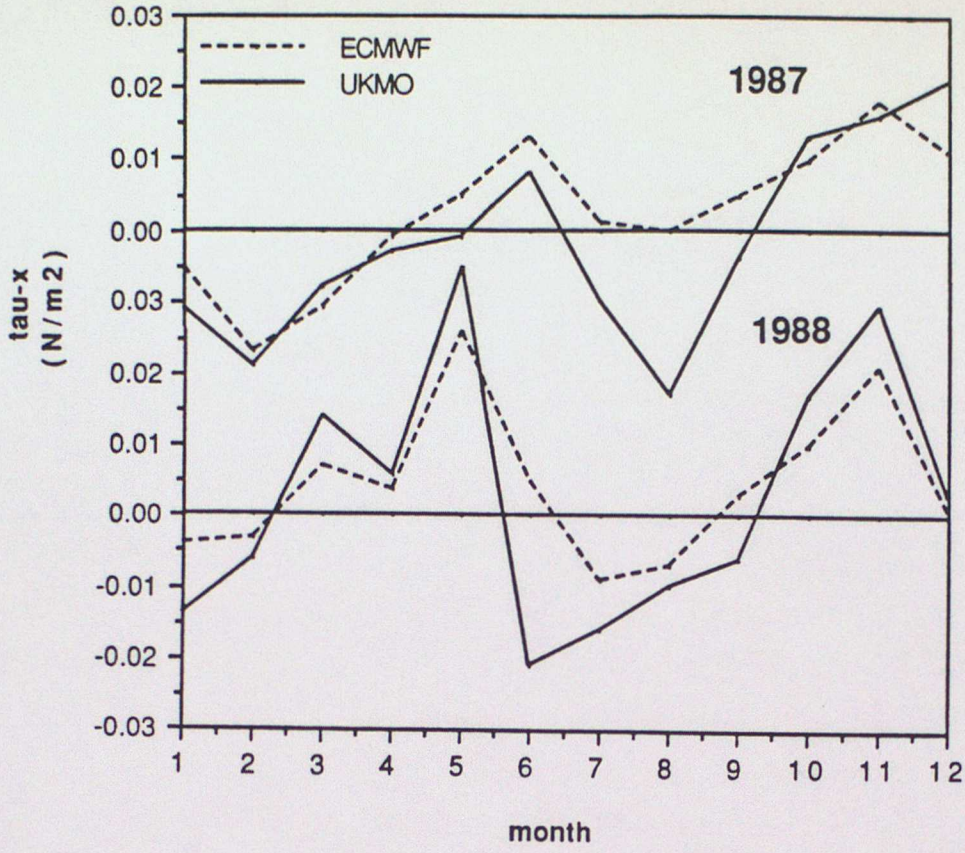

Fig. 10

Plot of the monthly mean zonal wind stress for 1987 and 1988 at 73°E from the UKMO (solid) and ECMWF (dashed) analyses. Both show similar interannual variations, with differences of typically less than 0.01 Nm^{-2}, but in Aug 87 and June 88 the differences are larger, up to 0.025 Nm^{-2}. The UKMO shows larger variability than ECMWF and shows stronger westward stresses, particularly in Northern Hemisphere summer.

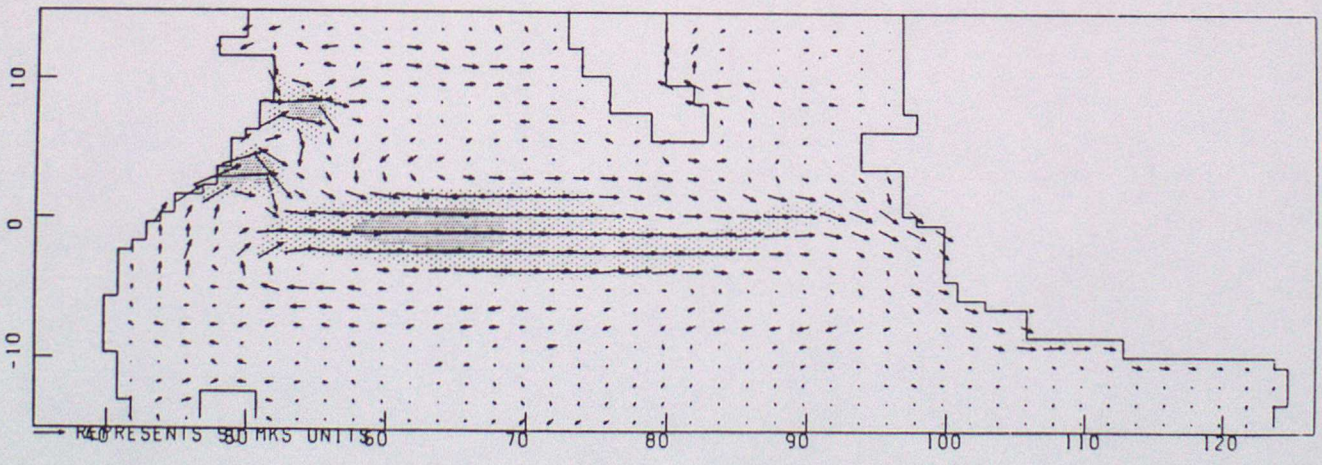

Fig. 11

Plot of the vector difference in surface currents between those obtained from ECMWF forcing and those from UKMO forcing (INDN-INDG), for July 1988. The differences are largest in the Somali current region and in the equatorial region, where they reach almost 1 ms^{-1}. Elsewhere differences in excess of 20 cms^{-1} are noted in the Arabian Sea, Bay of Bengal and in the South Equatorial current. The currents along the Somali coast exhibit a more pronounced 2-gyre structure in INDN than in INDG. Shading as for fig. 6.

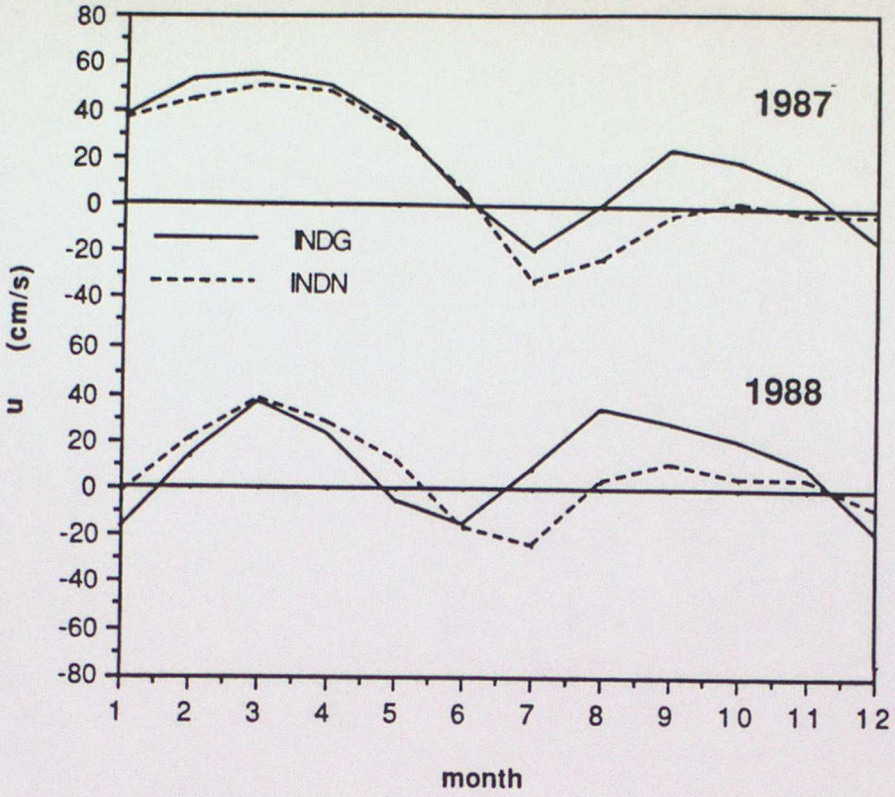

Fig. 12

Plot of zonal currents at 113 m at 73°E for INDG and INDN for 1987 and 1988. The currents are rather similar in the first 6 months of each year (see aso fig. 3), but show significant differences in the latter half of the year. The currents obtained using UKMO stresses show stronger eastward flow than the currents obtained using ECMWF or HR stresses. Both INDG and INDN show a semi-annual response, contrary to IND1 but consistent with observations shown in fig. 4.

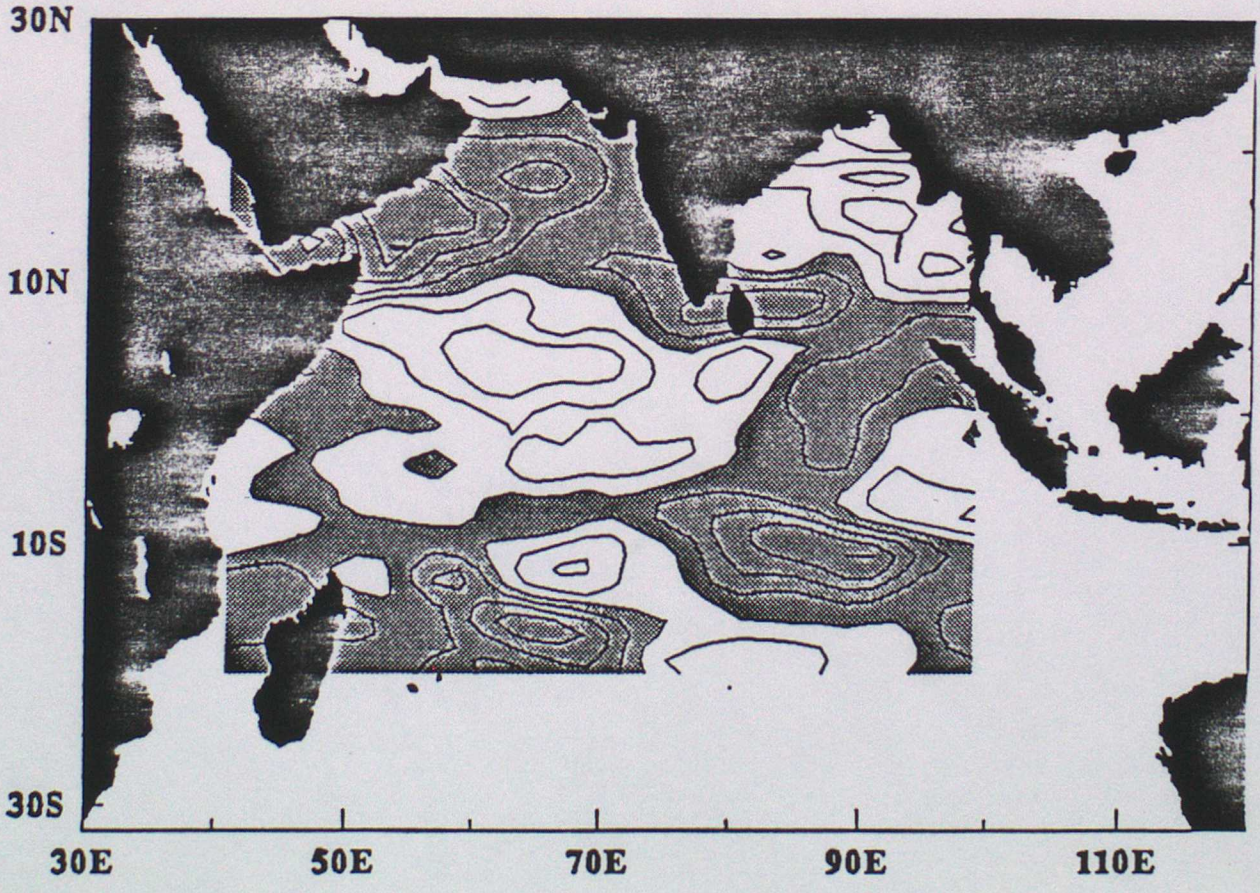

Fig. 13a

Deviation in surface topography from an annual mean as seen by GEOSAT. The contour interval is 4 cms. From CAC bulletin for July 1988.

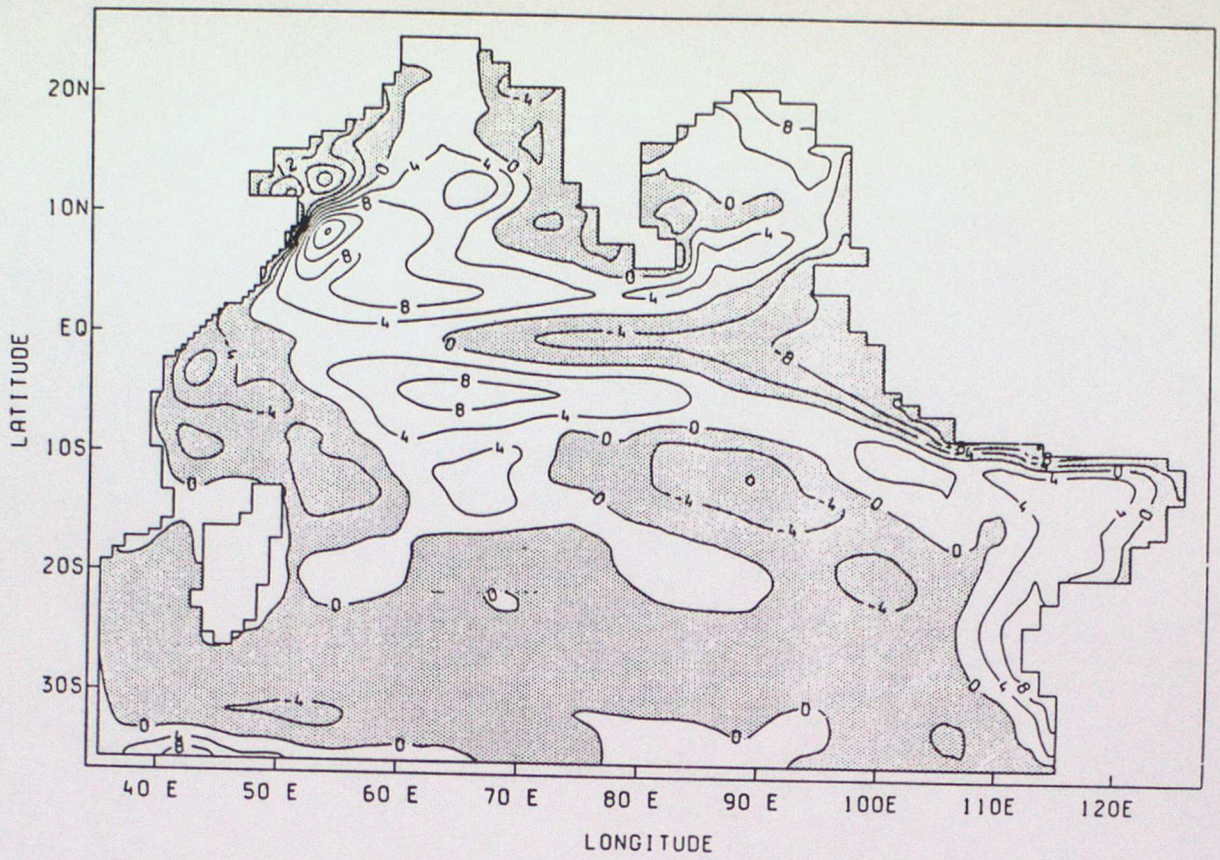

Fig. 13b **Deviation** of surface dynamic height relative to 800 m from an annual mean for INDG.

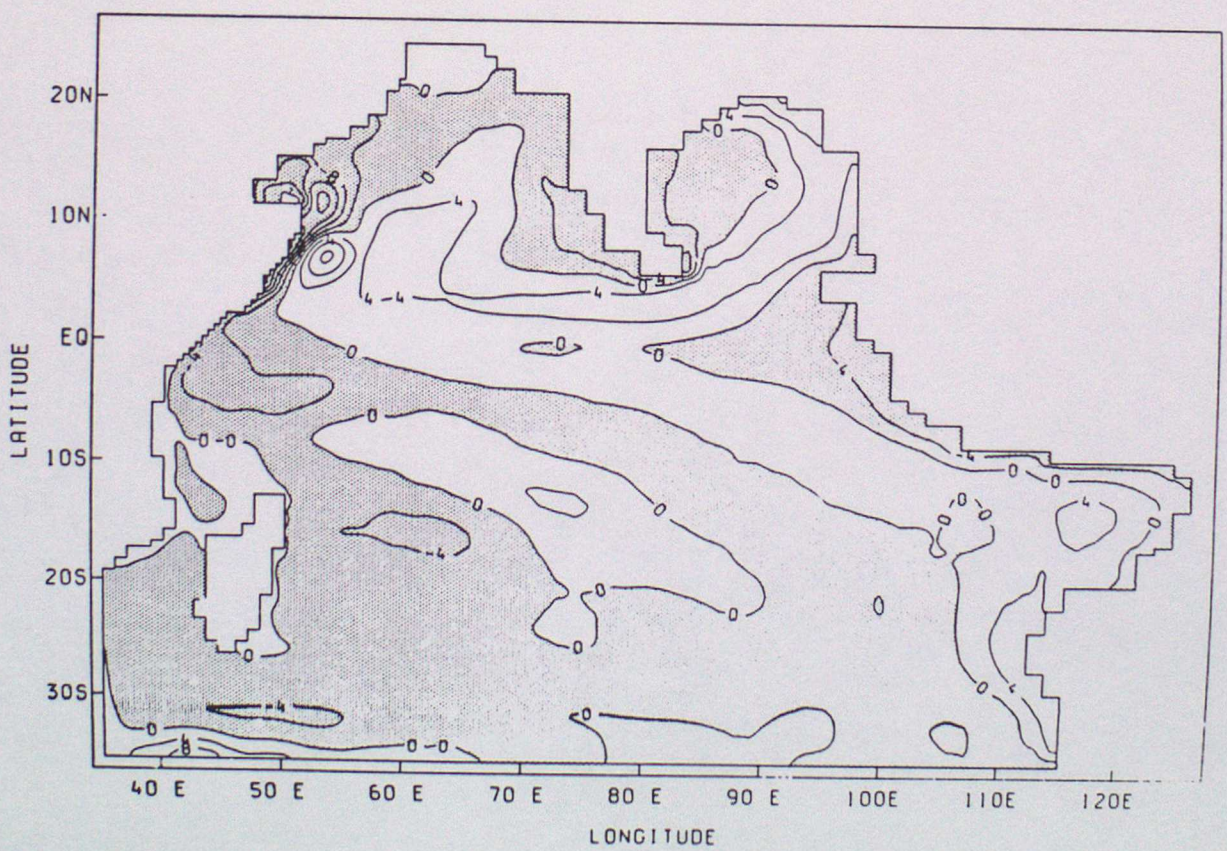

Fig. 13c As for fig. 13b, but for INDN.

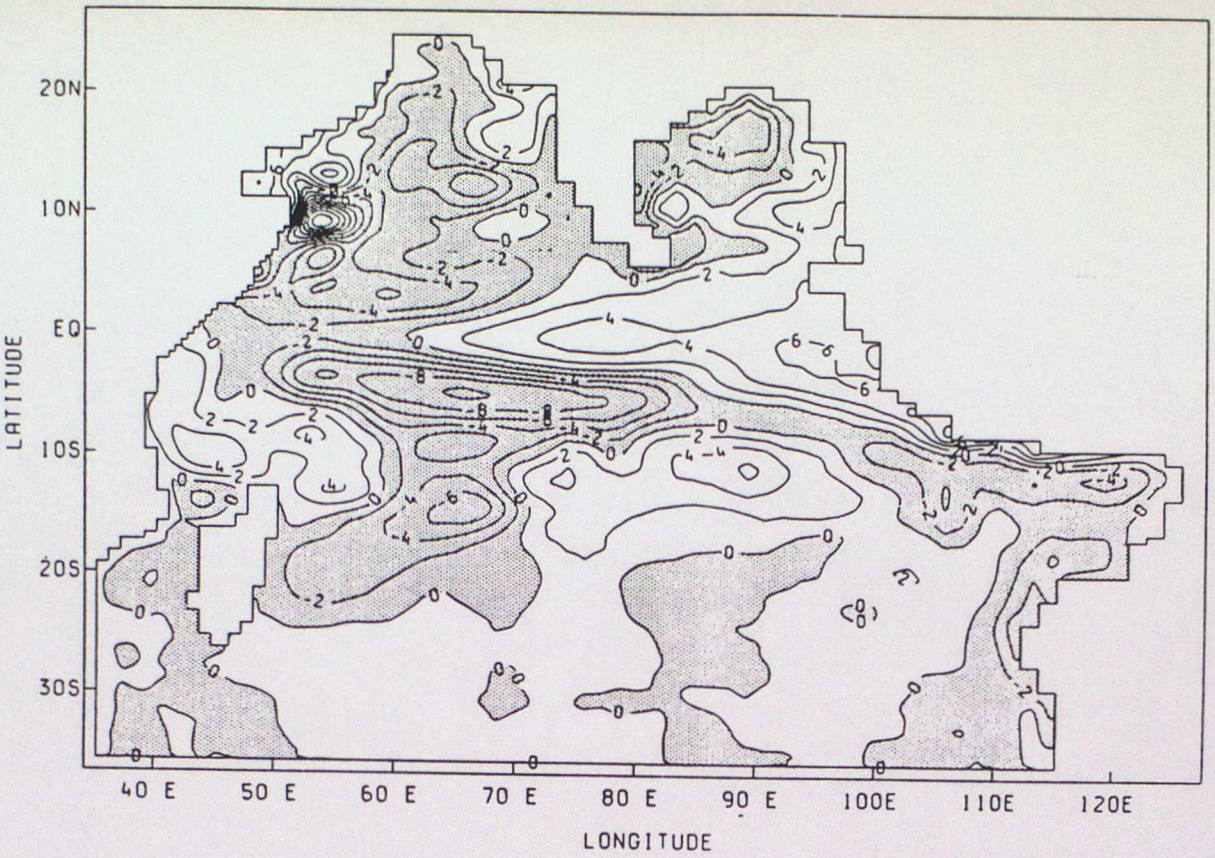

Fig. 13d

Differences in dynamic height for July 1988 (INDN–INDG). The contour interval is 4 dyn cms. Shading indicates negative values. Areas of large disagreement occur in the Somali gyre, in the south equatorial countercurrent at 5°S, at 15°S to the east of Madagascar, and in the eastern equatorial zone.

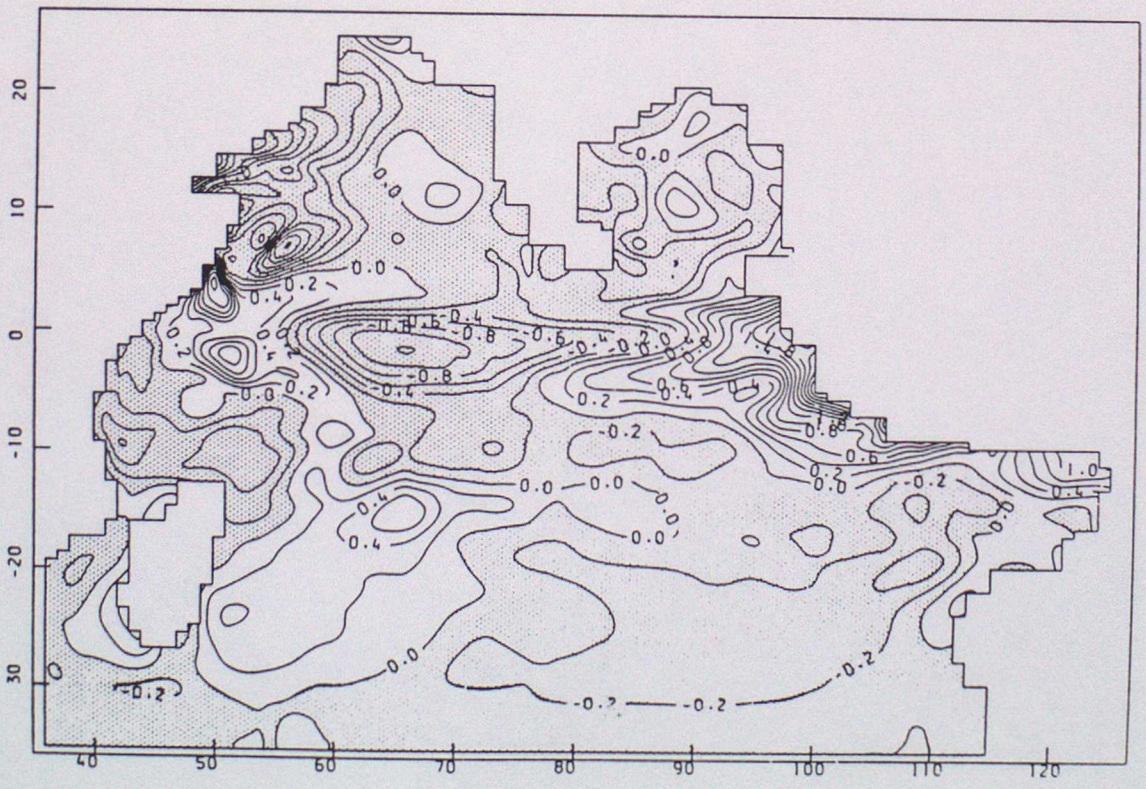

Fig. 14a

Differences in SST between July 1988 and July 1987 in the model integration INDG.

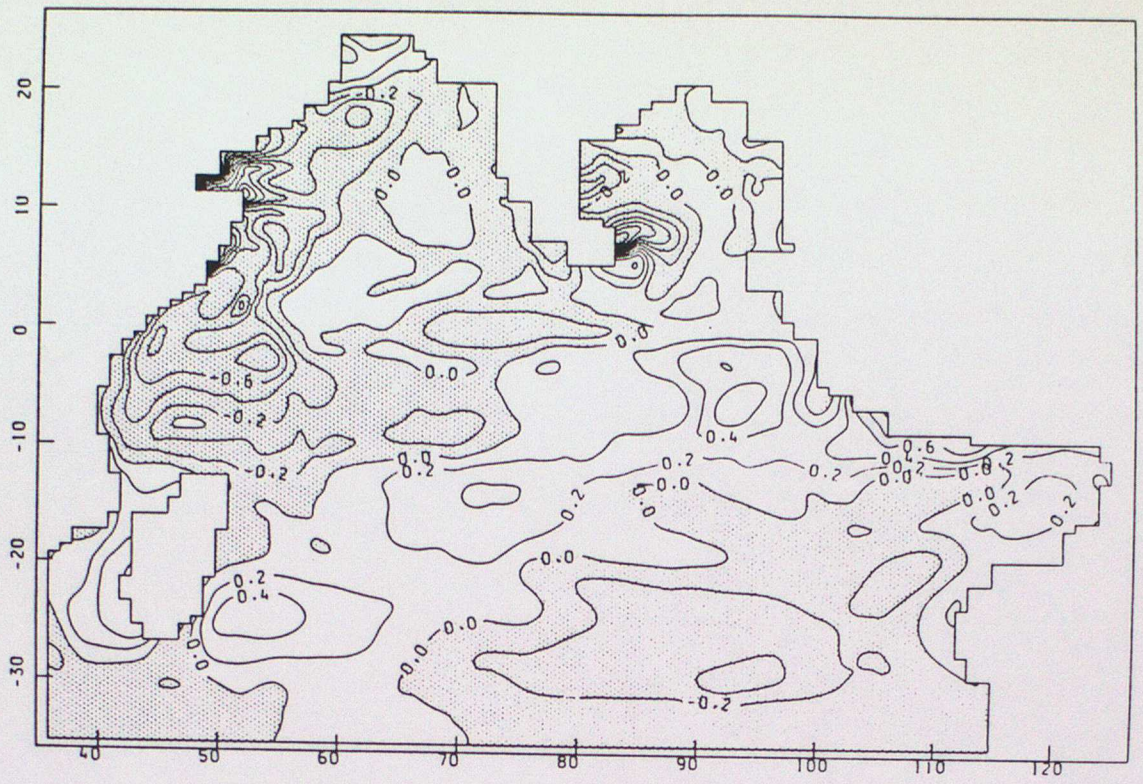

Fig. 14b As for fig. 14a. but for INDN.

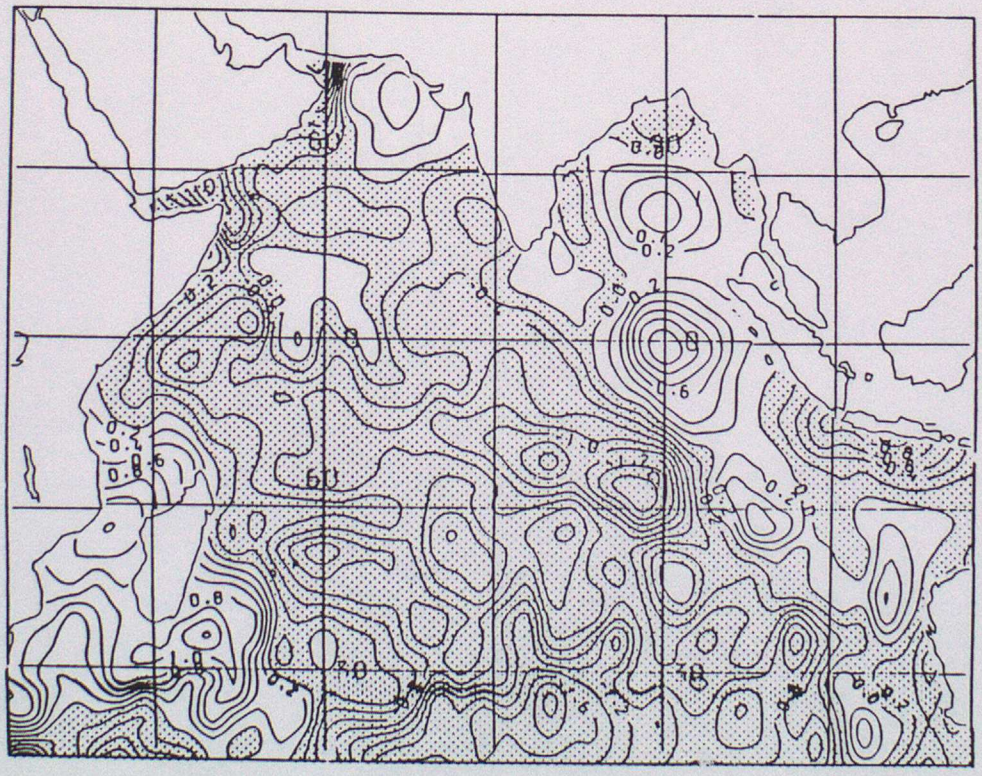

Fig. 14c Differences in SST between July 88 and July 87 from the CAC analyses. Neither model integration gives differences similar to observed, nor do the two model integrations agree.

CLIMATE RESEARCH TECHNICAL NOTES

CRTN 1	Oct 1990	Estimates of the sensitivity of climate to vegetation changes using the Penman-Monteith equation. P R Rowntree
CRTN 2	Oct 1990	An ocean general circulation model of the Indian Ocean for hindcasting studies. D J Carrington
CRTN 3	Oct 1990	Simulation of the tropical diurnal cycle in a climate model. D P Rowell
CRTN 4	Oct 1990	Low frequency variability of the oceans. C K Folland, A Colman, D E Parker and A Bevan
CRTN 5	Dec 1990	A comparison of 11-level General Circulation Model Simulations with observations in the East Sahel. K Maskell
CRTN 6	Dec 1990	Climate Change Prediction. J F B Mitchell and Qing-cun Zeng
CRTN 7	Jan 1991	Deforestation of Amazonia - modelling the effects of albedo change. M F Mylne and P R Rowntree
CRTN 8	Jan 1991	The role of observations in climate prediction and research. D J Carson
CRTN 9	Mar 1991	The greenhouse effect and its likely consequences for climate change. D J Carson
CRTN 10	Apr 1991	Use of wind stresses from operational N.W.P. models to force an O.G.C.M. of the Indian Ocean. D J Carrington
CRTN 11	Jun 1991	A new daily Central England Temperature series, 1772-1991. D E Parker, T P Legg and C K Folland
CRTN 12	Jul 1991	Causes and predictability of Sahel rainfall variability. D P Rowell, C K Folland, K Maskell, J A Owen, M N Ward
CRTN 13	Jul 1991	Modelling changes in climate due to enhanced CO_2, the role of atmospheric dynamics, cloud and moisture. C A Senior, J F B Mitchell, H Le Treut and Z-X Li

CLIMATE RESEARCH TECHNICAL NOTES

CRTN 14	Sep 1991	Sea temperature bucket models used to correct historical SST data in the Meteorological Office. C K Folland
CRTN 15	Aug 1991	Modelling climate change, and some potential effects on agriculture in the U.K. P R Rowntree, B A Callander and J Cochrane
CRTN 16	Aug 1991	The Boreal Forests and Climate G Thomas and P R Rowntree
CRTN 17	Aug 1991	Development of a Stratosphere-Troposphere Data Assimilation System. R Swinbank.
CRTN 18	Sep 1991	A study of asynchronous coupling using a simple climate model. M K Davey.
CRTN 19	Sep 1991	The Oceanic Carbon Cycle. N K Taylor
CRTN 20	Nov 1991	Worldwide ocean-atmosphere surface fields in Sahel wet and dry years using provisionally corrected surface wind data. M N Ward
CRTN 21	Dec 1991	Coupled tropical ocean global atmosphere models at the UKMO. M K Davey, C Gordon, S Ineson and S Lawrence
CRTN 22	Dec 1991	Empirical parameterisation of tropical ocean-atmosphere coupling. M Allen, M K Davey, D L T Anderson and P D Killworth
CRTN 23	Feb 1992	The temporal evolution of Equatorial Currents in the Indian Ocean D L T Anderson, D J Carrington, R A Corry and C Gordon
CRTN 24	Feb 1992	Stratospheric analyses provided by the U.K. Meteorological Office M J Bailey, A O'Neill and V D Pope
CRTN 25	Feb 1992	Modelling interannual variability in the Indian Ocean using momentum fluxes from the UKMO and ECMWF operational weather analyses. D L T Anderson and D J Carrington